

ISTANBUL TECHNICAL UNIVERSITY ★ ENERGY INSTITUTE

**HYDROGEN AND CARBON NANOTUBE PRODUCTION VIA CATALYTIC
DECOMPOSITION OF METHANE**

M.Sc. THESIS

Cansu DENİZ

Energy Science and Technologies

Energy Science and Technologies

JANUARY, 2014

ISTANBUL TECHNICAL UNIVERSITY ★ ENERGY INSTITUTE

**HYDROGEN AND CARBON NANOTUBE PRODUCTION VIA CATALYTIC
DECOMPOSITION OF METHANE**

M.Sc. THESIS

Cansu DENİZ

Energy Science and Technologies

Energy Science and Technologies

Thesis Advisor: Prof. Dr. Nilgün KARATEPE YAVUZ

JANUARY, 2014

İSTANBUL TEKNİK ÜNİVERSİTESİ ★ ENERJİ BİLİMLERİ ENSTİTÜSÜ

**METANIN KATALİTİK AYRIŞMASI İLE HİDROJEN VE KARBON NANOTÜP
ELDESİ**

YÜKSEK LİSANS TEZİ

**Cansu DENİZ
(301111005)**

Enerji Bilimi ve Teknolojileri Programı

Enerji Bilimi ve Teknolojileri Programı

Thesis Advisor: Prof. Dr. Nilgün KARATEPE YAVUZ

OCAK 2014

Cansu Deniz, a M.Sc. student of ITU Institute of Energy student ID 301111005, successfully defended the thesis entitled “ Hydrogen and Carbon Nanotube Production via Catalytic Decomposition of Methane ” which she prepared after fulfilling the requirements specified in the associated legislations, before the jury whose signatures are below.

Thesis Advisor : **Prof. Dr. Nilgün KARATEPE YAVUZ**
İstanbul Technical University

Jury Members :

Date of Submission : 16 December 2013
Date of Defense : 23 January 2014

To my family,

FOREWORD

Initially, I would like to thank my academic advisor Prof. Dr. Nilgün KARATEPE YAVUZ. This thesis would not have been possible without her inspiration and effort. I appreciate for her advice, encouragement and support throughout the study and writing this thesis.

I would like to thank also to Prof. Dr. Ali ATA and Ercan ÖZDEMİR for their helps and permissions to use hydrogen laboratory at Gebze Institute of Technology. I am also thankful to Dr. Eyüp ŞİMŞEK for his additive, helps, interest and support throughout this study. I am greatly indebted to Prof. Dr. Fikret Yüksel and Assis. Prof. M. Selçuk Mert, of Yalova University Energy System Engineering Department, for their invaluable support in allowing me sufficient time for completing my master thesis which required comprehensive experimental research.

Special thanks to Research Assist. Neslihan YUCA and Fatih GÜMÜŞ for their technical aid as well as their heartfelt friendship. I was very lucky to be a part of such a great team. I also would like to thank Research Assist. Aydın HAŞİMOĞLU, Özlem UÇAK and Mehbare BAHAR for their help and assistance with experiments in the laboratory. I am also thankful to Research Assist. Ezgi BAYRAKDAR for her support, valuable suggestions and encouragement during this study. I also want to thank Hakan ESGEL, MSc student at ITU, for his help and support. Many thanks to my friends from ITU Energy Institute, Yalova University Energy System Engineering Department and Gebze Institute of Technology Nano Technology Center for their helps, friendships and interest.

I also thankful to Gamze ÖZDEMİR and Sevgi SARI for their supports and friendships. I also want to thank my friend Zafer CANAL for his help, support, patience, encouragement and invaluable advices at hard times.

Finally, I am deeply thankful to my mum, Okşan, my father, Mehmet, my brother, Ahmet Eren for their love, support, and endless trust during my life.

December 2013

Cansu DENİZ
Environmental Engineer
Mechanical Engineer

TABLE OF CONTENTS

	<u>Page</u>
FOREWORD	ix
TABLE OF CONTENTS	xi
ABBREVIATIONS	xiii
LIST OF TABLES	xv
LIST OF FIGURES	xvii
HYDROGEN AND CARBON NANO TUBE PRODUCTION VIA CATALYTIC DECOMPOSITION OF METHANE	xix
METANIN KATALİTİK AYRIŞMASI İLE HİDROJEN ve KARBON NANOTÜP ELDESİ	xxi
1. INTRODUCTION	1
2. HYDROGEN	3
2.1 Properties of Hydrogen.....	3
2.1.1 Physical and chemical properties	3
2.1.2 Fuel properties.....	5
2.1.3 Energy content	5
2.1.4 Combustibility properties.....	6
2.2 Hydrogen Production Methods.....	7
2.3 Application Field of Hydrogen Energy	11
3. PRODUCTION OF HYDROGEN FROM HYDROCARBONS	13
3.1 Hydrocarbon to Hydrogen Technologies	13
3.2 Oxidative Processing of Hydrocarbons	14
3.2.1 Steam reforming	14
3.2.2 Partial oxidation	16
3.2.3 Auto thermal reforming.....	16
3.2.4 Carbon dioxide reforming of hydrocarbons	17
3.2.5 Steam iron process	17
3.2.6 Plasma reforming	18
3.2.7 Photo-production of hydrogen form hydrocarbons.....	18
3.3 Non-oxidative Processing of Hydrocarbons.....	18
3.3.1 Thermal decomposition of hydrocarbons	18
3.3.2 Catalytic decomposition of hydrocarbons.....	19
3.3.2.1 Literature studies	21
3.3.3 Plasma-assisted decomposition of hydrocarbons.....	27
4. EXPERIMENTAL STUDIES	29
4.1 Catalyst Preparation.....	29
4.2 Catalyst Characterization.....	30
4.3 Hydrogen and Carbon Nanotubes Production.....	31
5. RESULTS AND DISCUSSIONS	33
5.1 Catalyst Characterizations and Hydrogen Production Results	33
5.1.1 Nickel catalysts	34

5.1.2 Iron catalysts	36
5.1.3 Cobalt catalysts	37
5.2 The Effect of Reaction Temperature on Catalytic Decomposition of Methane	38
5.2.1 Nickel catalysts	38
5.2.2 Cobalt catalysts	42
5.2.3 Iron catalysts	45
5.3 The Effect of Catalysts Type on Catalytic Decomposition of Methane	48
5.4 The Effect of Substrate Types on Catalytic Decomposition of Methane	50
5.5 Carbon Production Results	52
5.5.1 XRD results	52
5.5.2 TGA results	56
5.5.3 SEM results	59
6. OVERALL RESULTS AND RECOMMENDATIONS.....	63
6.1 Concluding Remarks	63
6.2 Recommendations.....	65
REFERENCES.....	67
CURRICULUM VITAE.....	79

ABBREVIATIONS

ATR	: Auto thermal reforming
CNT	: Carbon Nanotube
GHG	: Green House Effect
NG	: Natural Gas
NO_x	: Nitrogen Oxides
PO_x	: Partial oxidation
SEM	: Scanning Electron Microscopy
SMR	: Steam Methane Reforming
SO_x	: Sulphur Oxides
SR	: Steam Reforming
TCD	: Thermal Catalytic Decompositon
TEM	: Transmission Electron Microscopy
TGA	: Thermal Gravimetric Analysis
VOC	: Volatile Organic Compound
XRD	: X-Ray diffraction

LIST OF TABLES

	<u>Page</u>
Table 2.1: Properties of hydrogen	4
Table 2.2: Volumetric and gravimetric energy density of different fuels	6
Table 2.3: Comparison of hydrogen with other fuels	8
Table 2.4: Estimated Cost of Hydrogen Production Transportation and Distribution...	10

LIST OF FIGURES

	<u>Page</u>
Figure 2-1 : Isotopes of hydrogen, protium, deuterium and tritium [11].....	3
Figure 2-2 : Hydrogen Production processes [17].	7
Figure 2-3 : Sources and Application areas [22].....	11
Figure 2-4 : Hydrogen car and bus [23-24].....	12
Figure 3-1 : World hydrogen production structure [20].	13
Figure 3-2 : (a) Theoretical energy consumption for hydrogen production from different feed stocks. (b) Maximum theoretical yield of hydrogen produced by steam reforming (gasification) of different feed stocks [2].	14
Figure 3-3 : Process flow diagram for hydrogen production by using steam-methane reforming SMR [5].....	15
Figure 3-4 : Thermodynamic equilibrium data for methane decomposition reaction at atmospheric pressure	19
Figure 3-5 : Summary of literature data on methane decomposition catalysts and preferred temperature range; Catalysts: 1 = nickel, 2 = iron, 3 = carbon, and 4 = other transition metals (Co, Pd, Pt, Cr, Ru, Mo) [2].	20
Figure 3-6 : Fixed and fluidized beds conversion at 550 °C. (G Ni/ γ Al ₂ O ₃ , A Ni/ α Al ₂ O ₃ , S Ni/SiO ₂).	24
Figure 3-7 : Schematic representation of carbon filaments of different structure produced by metal-catalyzed decomposition of methane. (a) Platelet structure, (b) “herringbone” structure, and (c) ribbon structure. MP denotes a nano-sized metal particle [2].	26
Figure 3-8 : The two growth modes of filamentous carbon.....	26
Figure 3-9 : SEM micrographs of the carbon nanostructures formed by CDM with each catalyst.	27
Figure 3-10 : TEM micrographs of the carbon nanostructures formed by CDM. A: Ni:Al ₂ O ₃ catalyst, B: Ni:Cu:MgO catalyst, C: Fe:Al ₂ O ₃ catalyst D: Fe:Mo:MgO catalyst.....	28
Figure 4-1 : (a) “Bandelin Sonoplus” sonicator (b) Catalysts during drying process. (c) Catalysts after grinding	30
Figure 4-2 : Schematic Diagram of Hydrogen Production System	31
Figure 4-3 : (a) Reactor system (b) Mass flow meter (c) Gas chromatography	32
Figure 5-1 : XRD patterns of Nickel catalysts after calcination process	34
Figure 5-2 : SEM-EDX images of Ni catalyst (a) Ni/SiO ₂ (b) Ni/MgO.....	35
Figure 5-3 : XRD patterns of Fe catalysts	36
Figure 5-4 : SEM images of Fe catalysts (a) Fe/SiO ₂ (b) Fe/MgO.....	36
Figure 5-5 : XRD patterns of Co catalysts.....	37
Figure 5-6 : SEM images of Co catalysts (a) Co/SiO ₂ (b) Co/MgO.....	38

Figure 5-7 : (a) Hydrogen production efficiency (%) (b) Methane conversion (%) for Ni/SiO ₂ catalyst at the reaction time of 3 h.....	39
Figure 5-8 : (a) Hydrogen production efficiency (%) (b) Methane conversion (%) for Ni/MgO catalyst at the reaction time of 3 h.	41
Figure 5-9: (a) Hydrogen production efficiency (%) (b) Methane conversion (%) for Co/SiO ₂ at the reaction time of 3 h.	42
Figure 5-10 : (a) Hydrogen production efficiency (%) (b) Methane conversion (%) for Co/MgO at the reaction time of 3 h.....	43
Figure 5-11: (a) Hydrogen production efficiency (%) (b) Methane conversion (%) for Fe/SiO ₂ at the reaction time of 3 h.	45
Figure 5-12: (a) Hydrogen production efficiency (%) (b) Methane conversion (%) for Fe/MgO at the reaction time of 3 h.....	47
Figure 5-13: (a) Hydrogen production efficiency (%) (b) Methane conversion (%) for Fe/SiO ₂ and Fe/MgO at 800°C and the reaction time of 3 h.	48
Figure 5-14: Hydrogen production efficiencies for all catalysts at 550°C.....	49
Figure 5-15: Hydrogen production efficiencies for all catalysts at 600°C.....	49
Figure 5-16: Methane conversions for all catalysts at 550°C	50
Figure 5-17: The effect of support materials on hydrogen production for Ni catalysts at 500°C	51
Figure 5-18: The effect of support on hydrogen production for Co catalysts at 550°C	52
Figure 5-19: XRD patterns of deactivated nickel catalysts at various temperatures	53
Figure 5-20: XRD patterns of deactivated cobalt catalysts at various temperatures	54
Figure 5-21: XRD patterns of deactivated iron catalysts at various temperatures....	55
Figure 5-22: TGA of carbon materials and carbon efficiency (%) for nickel catalysts	57
Figure 5-23: TGA of carbon materials and carbon efficiency (%) for cobalt catalysts	57
Figure 5-24: TGA of carbon materials and carbon efficiency (%) for iron catalysts	58
Figure 5-25: SEM images of CNTs synthesized using (a) Ni/SiO ₂ and (b) Ni/MgO catalysts	59
Figure 5-26: SEM images of CNTs synthesized using (a) Co/SiO ₂ and (b) Co/MgO catalysts	60
Figure 5-27: SEM images of CNTs synthesized using (a) Fe/SiO ₂ and (b) Fe/MgO catalysts	62
Figure 5-28: SEM images of CNTs synthesized using iron catalysts at the temperature of 800 °C	62

HYDROGEN AND CARBON NANO TUBE PRODUCTION VIA CATALYTIC DECOMPOSITION OF METHANE

SUMMARY

The future energy demand is expected to increase significantly due to an increasing world population and demands for higher standards of living and better air quality. Hydrogen is considered as an alternative energy carrier of the future to fossil fuels due to the harmful effects of NO_x, SO_x and VOC emissions to the environment. Furthermore, it has high conversion efficiency and low pollutant emissions. It can be produced from various sources by using different methods and transformed into electricity and other energy forms with a low pollution. Current world hydrogen production is approximately 50 million ton per year, which is equivalent to only 2% of world energy demand. Hydrogen can be produced from different feed stocks by using various processes. These include fossil fuel energy sources such as gasoline, coal and natural gas, and primary renewable and non-fossil energy sources such as solar, wind, nuclear, biomass, hydraulic and geothermal. When hydrogen is extracted from fossil hydrocarbon, all carbon dioxide must be processed (separated, sequestrated etc.). There are several methods to produce hydrogen from hydrocarbon sources such as steam reforming, partial oxidation, auto-thermal reforming. Steam reforming (SR) of natural gas (NG) is the most efficient and widely used process for the production of hydrogen. There is no by-product credit for the process and in the final analysis; it does not look environmentally friendly due to large CO₂ emissions. In partial oxidation and auto-thermal reforming processes a fuel, oxygen and steam are combined in proportions such that a fuel is converted into a mixture of H₂ and CO. Partial oxidation process can be carried out catalytically or non-catalytically. Catalytic decomposition of hydrocarbon is another method to produce hydrogen and it is also called non oxidative process that means no GHG emission or dangerous pollutants.

The objective of this study was to evaluate the impact of catalyst composition and processing parameters on CO_x-free hydrogen production and to produce an available solid form of co-product carbon as carbon nanotubes via catalytic decomposition of methane. Fe, Co and Ni are selected as catalysts over different substrates as SiO₂ and MgO to produce hydrogen at various temperatures (500°C-600°C). These catalysts were prepared by impregnation methods at İstanbul Technical University (ITU) – Energy Institute “Material Production and Preparation” laboratory. The catalytic decomposition experiments were carried out at GYTE Nano Technology Center Hydrogen Laboratory. Hydrogen production efficiencies and methane conversions of each catalyst were investigated. Product gases were hydrogen, methane and nitrogen and these gases have peaks that were determined by TCD3, FID and TCD1 detectors on gas chromatography respectively. Percentages of product gases were calculated by some empirical formulas using the peak areas which are proportional to amount of

the gas compounds. All data were recorded during 3 h of reaction time. Furthermore, the production of an available solid form of by-product carbon via catalytic decomposition of methane was investigated. Beside, catalysts and by-product carbon materials were investigated by XRD, TEM and SEM-EDX characterization techniques. All catalysts (Ni/SiO₂, Ni/MgO, Fe/SiO₂, Fe/MgO, Co/SiO₂, Co/MgO) have different conversion efficiency at various temperatures for hydrogen and carbon nanotube production and these results were compared with each other.

METANIN KATALİTİK AYRIŞMASI İLE HİDROJEN ve KARBON NANOTÜP ELDESİ

ÖZET

Geleceğin enerji ihtiyacının, artan nüfus, yüksek standartlarda yaşam gereksinimi ve daha temiz hava kalitesi için önemli bir ölçüde artması beklenmektedir. Hidrojen enerjisi, genellikle fosil yakıtların yanmasından kaynaklanan NO_x, SO_x ve VOC emisyonlarının çevreye verdikleri zararlı etkiden dolayı, geleceğin alternatif enerji taşıyıcısı olarak kabul edilmektedir. Daha da önemlisi, hidrojen enerji taşıyıcısıdır ve düşük kirletici emisyonu ile yüksek enerji dönüşüm verimine sahiptir. Dünyada, yıllık 50 milyon ton hidrojen üretilmekte ve bu sadece enerji ihtiyacının %2 sini karşılamaktadır. Hidrojen farklı yöntemlerle farklı kaynaklardan üretilerek diğer enerji formlarına ve elektriğe dönüştürülmektedir. Hidrojen enerjisinin kullanım alanları da son zamanlarda yaygınlaşmaya başlamıştır. Konvansiyonel güç sistemlerinde ve yakıt hücrelerinde hidrojen yakıt olarak kullanılmaktadır. Böylelikle daha temiz ve daha verimli bir enerji üretilmektedir. Ülkemizde de hidrojen ile ilgili birçok proje hayata geçirilmiştir. Hibrit enerji üretim sistemleri, yakıt hücresi kullanılarak çalıştırılan araçlar, botlar ve kesintisiz güç kaynakları, proje olmaktan çıkmış ve Unido-Ichet tarafından uygulamaları da gerçekleştirilmiştir. Dünyada da birçok örnekleri mevcuttur. NASA'nın uzay programında hidrojen yakıt hücresi kullanılmış, elektrik üretimi ve içme suyu üretimi gerçekleştirilmiştir.

Hidrojenin üretilmesi için kullanılan kaynaklar; fosil yakıtlar ve yenilenebilir fosil olmayan yakıtlar olarak sınıflandırılmaktadır. Kömür, doğalgaz gibi hidrokarbon içerikli yakıtlar fosil yakıtlar içine girerken, güneş, rüzgar, nükleer, biyo kütle ise fosil olmayan kaynaklardır. Hidrojen, hidrokarbon yakıtlardan elde edilirse, oluşan karbon dioksit gazı gibi sera etkisi yaratacak gazlar giderilmelidir. Hidrokarbonlardan hidrojen üretimi çeşitli yöntemler kullanılarak gerçekleştirilmektedir. Buhar reformasyonu ve kısmi oksidasyon en çok kullanılan yöntemler olup buhar reformasyonu en verimli yöntemdir. Ancak, karbon dioksit salınımı gerçekleştiğinden çevreci bir yaklaşım olduğu söylenemez. Kısmi oksidasyon yöntemi ile hidrojen üretimi sırasında da karbondioksit açığa çıkarmaktadır. Her iki yöntem de oksidatif reaksiyonlar içerir. Oksidatif olmayan yöntemlerden, hidrokarbonların katalitik ayrışması çevreci süreç olarak bilinir. Ürün olarak, hidrojen ve katı karbon oluşmaktadır. Hidrojen üretimi için gerekli olan enerji ihtiyacı, buhar reformu için gerekli olandan daha azdır. Hidrokarbon olarak genellikle doğal gaz veya metan kullanılmaktadır. Doğal gaz, hidrojen üretiminde en az enerjiye ihtiyacı olan ve hidrojen verimi yüksek olan bir yakıttır. Doğal gazın yaklaşık olarak %90'ı metandır. Metanın katalitik ayrışması endotermik tek bir reaksiyon ile gerçekleşmekte ve başka bir reaksiyona ihtiyaç duyulmamaktadır. Bu yöntemde, aktivasyon enerjisini düşürmek için katalizörler kullanılmaktadır. Ayrıca katalitik olmayan yöntemlere göre daha düşük sıcaklıklar da çalışılması sağlanır. Demir

(Fe), nikel (Ni), kobalt (Co) gibi katalizörler, silika, MgO, TiO₂ ya da alümina gibidestek malzemesi ile birlikte farklı yöntemler kullanılarak hazırlanmaktadır. Her katalizör için çalışılacak bir sıcaklık aralığı söz konusudur. Kullanılan katalizör dışında hidrojen üretimi prosesine etki eden birçok değişken de bulunmaktadır. Bu değişkenler; ısı kaynağı, sıcaklık, reaktör çeşidi, katalizör tanecik boyutu, katalizöre uygulanan ön işlemler, katalizör hazırlama yöntemleri ve destek malzemesi olarak sayılabilir. Ayrıca, reaksiyon sırasında, reaktörde tıkanmalar gerçekleşebilir ve bu durum hidrojen üretimini olumsuz etkileyebilir. Reaktördeki tıkanma, katı karbon oluşumundan kaynaklanmaktadır ve katalizörün aktifliğinin sona erdiğinin göstergesidir.

Bu çalışmanın amacı, farklı katalizörler kullanarak metanın katalitik ayrışması ile CO₂ içermeyen hidrojen üreterek proses parametrelerini incelemek ve yan ürün olarak katı karbon üretmek ve malzeme özelliklerini karakterizasyon cihazları kullanarak belirlemektir. Hidrokarbon kaynağı olarak metan kullanılmıştır. Metandan hidrojen üretiminde, katalizör olarak Fe, Co ve Ni, destek malzemesi olarak ise SiO₂ ve MgO seçilmiştir. Katalizörler, destek malzemesi içinde ağırlıkça % 10 olacak şekilde emdirme yöntemi kullanılarak İstanbul Teknik Üniversitesi-Enerji Enstitüsü “Malzeme üretimi ve hazırlanması” laboratuvarında hazırlanmıştır. Metanın katalitik ayrışma deneyleri ise, Gebze Yüksek Teknoloji Enstitüsü, “Nano Teknoloji Merkezi”nde hidrojen laboratuvarındaki mevcut kurulu sistemde gerçekleştirilmiştir. Katalitik ayrışma deneylerinden önce, katalizörlere kalsinasyon ve indirgeme gibi ön işlemler uygulanmıştır. Kalsinasyon işlemi ile katalizörler oksit forma, indirgeme işlemi ise hidrojen gazı uygulanarak oksit formdaki katalizörler aktif metal formuna dönüştürülmektedir. Kalsinasyon işlemi 500°C’de 4 saat süreyle, indirgeme işlemi ise 400°C’de 2 saat süreyle uygulanmıştır. Ön işlemler sona erdikten sonra, sisteme 50 ml/dakika akış debisinde metan: azot (4:1) gaz karışımı beslenmiştir. Reaktör olarak sabit yataklı paslanmaz çelik reaktör, ısıtıcı olarak da elektrikli fırın kullanılmıştır. Reaksiyon süresi 3 saat olarak seçilmiştir. Katalitik ayrışma reaksiyonları, her bir katalizör için 3 farklı sıcaklıkta (500, 550 ve 600°C) gerçekleştirilmiş ve bu sıcaklıklardaki hidrojen üretim verimleri ve metan dönüşüm yüzdeleri tespit edilmiştir. Ayrıca, katalizör hazırlamada kullanılan farklı destek malzemelerinin hidrojen verimine etkisi de incelenmiştir. Hidrojen, metan ve azot gazlarının yüzdeleri, gaz kromatografisi de TCD3, FID ve TCD1 detektörleri ile belirlenen piklerin alanları ile ampirik formül kullanılarak hesaplanmıştır. Ayrıca, yan ürün olarak katı karbon oluşumu gözlemlenmiştir. Karbonun malzeme özellikleri araştırılmıştır, karakterizasyonu gerçekleştirilmiştir. Aynı zamanda katalizörlerin de karakterizasyonları XRD, TEM ve SEM-EDX teknikleri kullanılarak gerçekleştirilmiştir. Tüm katalizörlerin (Ni/SiO₂, Ni/MgO, Fe/SiO₂, Fe/MgO, Co/SiO₂, Co/MgO), farklı sıcaklıklarda farklı dönüşüm verimlerine sahip olduğu tespit edilmiş ve birbirleriyle karşılaştırılmaları yapılarak değerlendirilmiştir.

1. INTRODUCTION

Hydrogen is the most available and smallest element in the universe, however it can be found as compound [1]. Hydrogen has the highest energy content (per unit mass) than other fuels. For instance, hydrogen has about three times the energy content of gasoline (140.4 MJ/kg versus 48.6 MJ/kg). However, it has storage problem because of having low volumetric density and molecular size [2]. Hydrogen is essentially an energy carrier and environmentally attractive fuel [3]. Therefore, it can be considered as an alternative fuel in today's world. Using hydrogen as fuel could significantly reduce many environmental problems. For the past many years, environmentalists and several industrial organizations have promoted hydrogen fuel as the solution to the problems of air pollution and global warming [2-3]. After producing hydrogen, it can be used for many applications, but main obstacle for this is storage. Therefore, this problem prevents hydrogen usage. Another challenge is that hydrogen production is very costly process. If these challenges is overcome, the usage and production of hydrogen can be increased.

Hydrogen can be produced from various feed stocks using different methods. One of the most attractive sources is hydrocarbons to produce hydrogen. Using hydrocarbon fuels has many advantages such as their availability, relatively high H/C ratio, convenience of storage and distribution. Natural gas is the most popular hydrocarbon source, because it has high potential of hydrogen yield. Hydrogen production methods by using hydrocarbon as a source are examined into two processes which are oxidative and non-oxidative [3]. Common oxidative processes are steam reforming and partial oxidation processes. The most common hydrogen production method is steam methane reforming (SMR) process that is among major producers of CO₂ emissions [4]. In order to eliminate environmental effect of steam reforming, CO₂ should be captured and sequestered. However, additional step cause increasing

the cost of production [5]. The partial oxidation process is another major method to produce hydrogen. In partial oxidation (POX), the primary hydrocarbon fuel reacts with oxygen in an inadequate quantity for CO-producing combustion. The non-oxidative method that is examined in this paper is “catalytic decomposition”. Catalytic decomposition of hydrocarbons such as methane is an environmentally attractive, one-step process to produce hydrogen and solid form of carbon [6-7]. Methane decomposition reaction is moderately endothermic process. The energy requirement per mole of hydrogen produced (8.9 kcal/mole H₂) [5]. In this process, metal or carbon based catalysts are used to decrease reaction temperature and activation energy. It has been reported that the rate of methane decomposition activity by the transition metals follows the order: Co, Ru, Ni, Rh > Pt, Re, Ir > Pd, Cu, W, Fe, Mo [8].

This thesis deals with the performance of different catalysts (Fe, Co and Ni) using two support materials (MgO and SiO₂) in the catalytic decomposition of methane at various temperatures ranges (500-600 °C). Fe, Co and Ni were prepared by impregnation method at ITU Energy Institute “Material Production and Preparation” Laboratory using textural promoters of SiO₂ and MgO. The catalytic decomposition experiments were carried out at GYTE Nano Technology Center Hydrogen Laboratory. Hydrogen production efficiencies and methane conversions of each catalyst were investigated. Product gases were hydrogen, methane and nitrogen and these gases have peaks that were determined by TCD3, FID and TCD1 detectors on gas chromatography respectively. Percentages of product gases were calculated by some empirical formulas using the peak areas which are proportional to amount of the gas compounds. All data were recorded during 3 h of reaction time. Furthermore, solid form of by-product carbon as carbon nanotubes via catalytic decomposition of methane was investigated. All catalysts (Ni/SiO₂, Ni/MgO, Fe/SiO₂, Fe/MgO, Co/SiO₂, Co/MgO) have different conversion efficiency at various temperatures for hydrogen and carbon nanotube production and these results were compared with each other.

2. HYDROGEN

2.1 Properties of Hydrogen

2.1.1 Physical and chemical properties

Hydrogen atom is the lightest element which contains a single positively charged proton and a single negatively charged electron bound to the nucleus [9]. It has an atomic number of 1 and an atomic weight of 1.00797. It can be found as compound in the universe. Hydrogen exists as a compound with other elements such as carbon, oxygen and nitrogen. It is a major constituent of water and all organic matters, and is widely distributed not only on the earth but also throughout the Universe [10].

Hydrogen has three naturally occurring isotopes as shown in Figure 2-1, denoted ^1H (protium), ^2H (deuterium) and ^3H (tritium). Other, highly unstable nuclei (^4H to ^7H) have been synthesized in the laboratory but not observed in nature [11]. Protium is the most common hydrogen isotope with an abundance of more than 99.98%. Deuterium is the other stable isotope of hydrogen and its abundance is approximately 0.02%. Tritium is radioactive and occurs in nature very small amounts but may be produced artificially by various nuclear reactions.

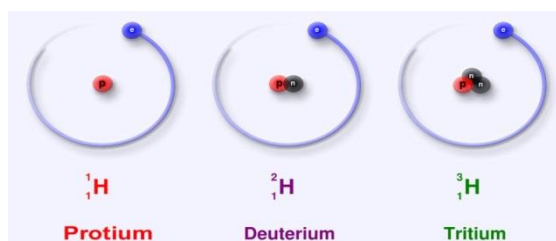


Figure 2-1 : Isotopes of hydrogen, protium, deuterium and tritium [11].

Hydrogen is a mixture of ortho- and para-hydrogen in equilibrium. If nuclear spins parallel, it is named as “ortho-hydrogen” however if nuclear spins anti parallel, it is

named as “para-hydrogen”. These two forms of hydrogen have differences on physical properties but chemical properties are same. At an ambient temperature, the normal hydrogen contains 75% ortho-hydrogen and 25% para-hydrogen. The ortho-to-para conversion is associated with the release of heat [12].

Hydrogen is colorless, odorless and tasteless. It is approximately 14 times lighter than air and diffuses faster than any other gas. Hydrogen has boiling temperature at -253 °C and melting temperature at -259 °C. The properties of hydrogen are summarized in Table 2.1. Solid metallic hydrogen has a greater electrical conductivity than any other solid elements. Moreover, the gaseous hydrogen has one of the highest heat capacity (14.4 kJ/kg.K).

Table 2.1 : Properties of hydrogen [10].

Property	Value
Molecular weight	2.01594
Density of gas at 0°C and 1 atm	0.08987 kg/m ³
Density of solid at -259°C	858 kg/m ³
Density of liquid at -253°C	708 kg/m ³
Melting temperature	-259°C
Boiling temperature at 1 atm	-253°C
Critical temperature	-240°C
Critical pressure	12.8 atm
Critical density	31.2 kg/m ³
Heat of fusion at -259°C	58 kJ/kg
Heat of vaporization at -253°C	447 kJ/kg
Thermal conductivity at 25°C	0.019 kJ
Heat capacity(Cp) of gas at 25°C	14.4 kJ/(kg.°C)
Heat capacity(Cp) of liquid at -256°C	8.1 kJ/(kg.°C)
Heat capacity(Cp) of solid at -259.8°C	2.63 kJ/(kg.°C)

At normal temperatures, hydrogen is nonreactive however hydrogen atom is chemically very reactive. Dissociation of hydrogen into atomic hydrogen requires very high temperatures. Naturally, the hydrogen is bound to either oxygen or carbon atoms. Moreover, energy expenditure is needed to obtain hydrogen from natural compounds. Atomic hydrogen is a powerful reducing agent at room temperature. Some salts, such as nitrates, nitrites and cyanides of sodium and potassium are

reduced to metallic state by atomic hydrogen. The product of hydrogen reacting with oxygen to generate energy is water vapor. At room temperature this reaction is slow however when catalysts are used, the reaction is accelerated.

2.1.2 Fuel properties

Fossil fuel energy resources are used for our current energy system however it is not long lasting solution to the problems of stationary energy supply and supply with fuel for transportation. Moreover, using fossil fuel energy resources lead to many environmental problems such as emissions of harmful substances and greenhouse effects. Nowadays, these problems are rapidly gaining importance [13].

Hydrogen is found in water and many organic compounds, notably the “hydrocarbons” that make up many of our fuels such as gasoline, natural gas, methanol and propane. Hydrogen can be separated from these compounds by using several processes. Hydrogen is highly flammable over a wide range of temperature and concentration. Moreover, it will become a major energy resource if some challenges are overcome. Hydrogen is currently more expensive than conventional energy sources; the production efficiency must be improved and an infrastructure to transport and distribute hydrogen must be developed [14].

2.1.3 Energy content

Hydrogen has the highest energy content per unit mass and the lowest energy content per unit volume according to other fuels as shown in

Table 2.2. For instance, on a weight basis, hydrogen has three times the energy content of gasoline. However, on volume basis, gasoline has higher energy density than hydrogen. Having low volumetric density causes in storage problem for hydrogen. For automobile applications, a large container is needed to store adequate hydrogen for an enough driving range. The energy density of hydrogen is also affected by the physical nature of the fuel, whether the fuel is stored as a liquid or as a gas; and if a gas, at what pressure [2].

Table 2.2 : Volumetric and gravimetric energy density of different fuels [1].

Fuel	Volumetric Energy Density (MJ/m³ of liquid)	Gravimetric Energy Density (MJ/kg)
Hydrogen	8,491	140.4
Methane	20,920	43.6
Propane	23,488	28.3
Gasoline	31,150	48.6
Diesel	31,435	33.8
Methanol	15,800	20.1

2.1.4 Combustibility properties

Hydrogen is flammable in 4-75% concentrations however gasoline has 1.3-7.1% concentrations range as shown in Table 2.3. Defining equivalence ratio in terms of flammability is more meaningful for internal combustion engines. Equivalence ratio (ϕ) defined as the mass ratio of actual fuel/air ratio to the stoichiometric fuel/air ratio. The flammability range for hydrogen is $0.1 < \phi < 7.1$, and that for gasoline is $0.7 < \phi < 4$. This shows that hydrogen internal combustion engine is available to stable operation even under highly dilute conditions. However, the wider range gives additional control over the engine operation for emissions and fuel metering. The final combustion temperature is generally lower with hydrogen fuel than with gasoline, reducing the amount of pollutants, such as NO_x , emitted in the exhaust [15].

Hydrogen has low ignition energy and it enables hydrogen engines to provide prompt ignition even for lean mixtures. However, having low ignition energy means that hot gases and hot spots on the cylinder can serve as sources of ignition, creating problems of premature ignition and flashback.

The auto ignition temperature is the minimum temperature required to start self-sustained combustion in a combustible fuel mixture in the absence of an external ignition. For hydrogen, the auto-ignition temperature is relatively high as 585°C . This makes it difficult to ignite a hydrogen–air mixture on the basis of heat alone without some additional ignition source.

At stoichiometric ratio, hydrogen has higher flame speed than gasoline. Hydrogen engines can approach the thermodynamic engine cycle because of its flame speed. Moreover, having low density and high diffusivity, hydrogen dispersion in air is considerably faster than gasoline. There are two main reasons to become advantageous. First, high dispersion causes the formation of uniform mixture of fuel and air. Second reason is that if a hydrogen leak develops, hydrogen disperses out rapidly. Therefore, dangerous conditions can be avoided or minimized.

2.2 Hydrogen Production Methods

Current world hydrogen production is approximately 50 million ton per year, which is equivalent to only 2% of world energy demand. Hydrogen can be produced from different feed stocks by using various processes as shown in Figure 2-2. These include fossil fuel energy sources such as gasoline, coal and natural gas, and primary renewable and non-fossil energy sources such as solar, wind, nuclear, biomass, hydraulic and geothermal. Each method is in a different stage of development, and each offers unique opportunities, benefits and challenges. Local availability of feedstock, the maturity of the technology, market applications and demand, policy issues, and costs will all influence the choice and timing of the various options for hydrogen production [16].

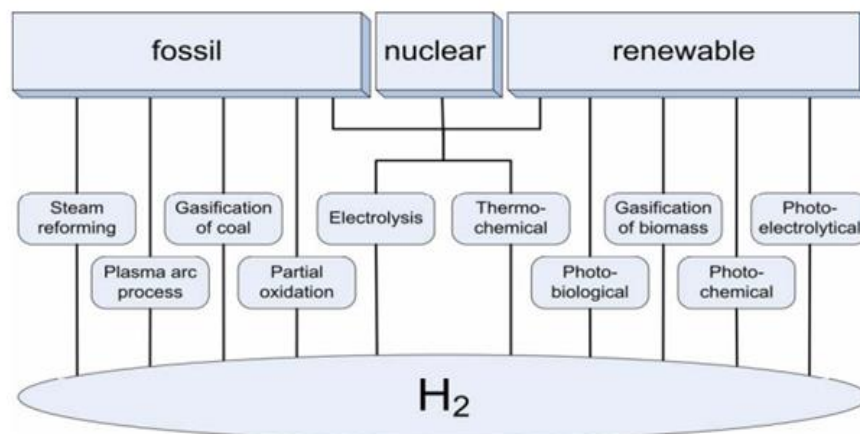


Figure 2-2 : Hydrogen Production processes [17].

Table 2.3 : Comparison of hydrogen with other fuels [1].

Fuel	LHV (MJ/kg)	HHV (MJ/kg)	Stoichiometric air/fuel ratio(kg)	Combustible Range (%)	Flame Temp. (°C)	Min. Ignition Energy(MJ)	Auto- Ignition Temp. (°C)
Methane	50.0	55.5	17.2	5-15	1914	0.30	540-630
Propane	45.6	50.3	15.6	2.1-9.5	1925	0.30	450
Octane	47.9	15.1	0.31	0.95-6.0	1980	0.26	415
Methanol	18.0	22.7	6.5	6.7-36.0	1870	0.14	460
Hydrogen	119.9	141.6	34.3	4.0-75.0	2207	0.017	585
Gasoline	44.5	47.3	14.6	1.3-7.1	2307	0.29	260-460
Diesel	42.5	44.8	14.5	0.6-5.5	2327	-	180-320

When hydrogen is extracted from fossil hydrocarbon, all carbon dioxide must be processed (separated, sequestered etc.) such that no GHG or other pollutants are emitted in the atmosphere and the hydrogen extraction process can be called “green” [18]. There are several methods to produce hydrogen from hydrocarbon sources such as steam reforming, partial oxidation, auto-thermal reforming. Steam reforming (SR) of natural gas (NG) is the most efficient and widely used process for the production of hydrogen. The theoretical energy requirement per mole of hydrogen produced for the overall process is equal to 40.75 kJ/mole H₂. There is no by-product credit for the process and, in the final analysis; it does not look environmentally friendly due to large CO₂ emissions. The total CO₂ emissions from SR process reach up to 0.3-0.4 m³ CO₂ per each m³ of hydrogen produced. In partial oxidation and auto-thermal reforming processes a fuel, oxygen and steam are combined in proportions such that a fuel is converted into a mixture of H₂ and CO. Partial oxidation process can be carried out catalytically or non-catalytically. The maximum theoretical concentration of hydrogen in the effluent gas using pure oxygen is 66.7 v. %, however, the concentration drops to 40.9 v. % if air is used as an oxidizer. Amount of CO₂ produced by partial oxidation process depends on the composition of the feedstock used and could reach up to 0.5 m³ CO₂ per each m³ of hydrogen produced [17].

In addition to this, gasification method is used to get hydrogen from coal. Moreover, water electrolysis is the process whereby water is splitted into hydrogen and oxygen through the application of electrical energy, as in Eqn. 2.1 [16].



Catalytic decomposition of methane is another method to obtain hydrogen from hydrocarbons and it is called non-oxidative process that means no GHG emission or dangerous pollutants. Catalysts are used for this process because the use of a catalyst is extremely advantageous since the non-catalytic thermal decomposition would require elevated process temperatures, i.e., above 1200 °C [19].

A typical cost analysis for hydrogen production and distribution from different feedstocks is given in Table 2.4. The cost estimation is based on the energy content of a gallon of gasoline and a kilogram of hydrogen are approximately equal on a lower heating value basis. Thus, a kilogram of hydrogen is approximately equal to a gallon of gasoline equivalent (gge) on an energy content basis [2].

Table 2.4 : Estimated Cost of Hydrogen Production Transportation and Distribution [20].

Primary Energy Source	Production Cost (\$/kg)	Distribution Cost via Pipeline (\$/kg)	Dispensing Cost (\$/kg)	Total Cost (\$/kg H₂)
Natural Gas Reforming	1.03	0.42	0.54	1.99
Natural gas + CO₂ capture	1.22	0.42	0.54	2.17
Coal Gasification	0.96	0.42	0.54	1.91
Coal + CO₂ capture	1.03	0.42	0.54	1.99
Wind electrolysis	6.64	0.42	0.54	7.60
Biomass Gasification	4.63	1.80	0.62	7.04
Biomass pyrolysis	3.80	1.80	0.62	6.22
Nuclear thermal splitting of water	1.63	0.42	0.54	2.33
Gasoline (for reference)	0.93\$/gal.refined	0.19 \$	-	1.12\$/gal

2.3 Application Field of Hydrogen Energy

Hydrogen can be used in conventional power generation technologies, such as automobile engines and power plant turbines, or in fuel cells, which are relatively cleaner and more efficient than conventional technologies. Fuel cells are devices that directly convert hydrogen into electricity. Thus, fuel cells have wide application potential in both transportation and electrical power generation, including on-site generation for individual homes and office buildings called as stationary applications [14]. Current thinking suggests that fuel cells are the path for the use of hydrogen and that the fuel cell industry is driving the hydrogen economy [21]. It is also used in NASA's space program as fuel for the space shuttles, and in fuel cells that provide heat, electricity and drinking water for astronauts [14].

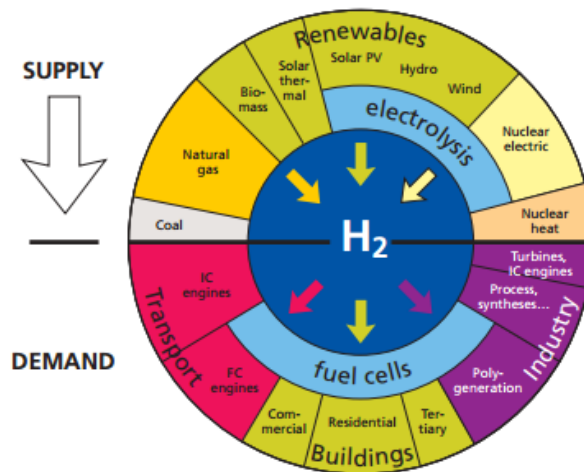


Figure 2-3 : Sources and Application areas [22].

Today, hydrogen is used primarily in ammonia manufacture, petroleum refinement and synthesis of methanol. Transportation applications for hydrogen include buses, trucks, passenger vehicles, and trains. Technologies are being developed to use hydrogen in both fuel cells and internal combustion engines, including methanol systems. Hydrogen cars may be a great idea for future.

Hydrogen cars and fuel cells are often promoted as being potentially emission-free if they burn hydrogen, in contrast to currently more common fuels such as methane or natural gas that generate carbon dioxide. Moreover, hydrogen is used in buses as shown in Figure 2-4. The BMW Clean Energy World Tour 2002 presented the hydrogen technology and the hydrogen internal combustion engine to leading

opinion leaders and decision makers from politics, industry and science. The goal was to establish a hydrogen infrastructure through global partnerships in order to cause the breakthrough of the fuel of the future.

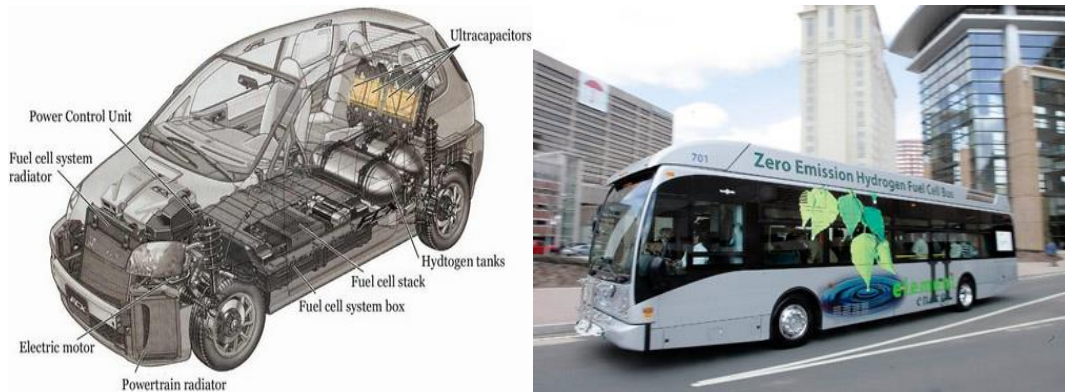


Figure 2-4 : Hydrogen car and bus [23-24].

In addition, stationary power applications include back-up power units, grid management, power for remote locations, stand-alone power plants for towns and cities, distributed generation for buildings and cogeneration. In general, combustion-based processes, such as gas turbines and reciprocating engines, can be designed to use hydrogen either alone or mixed with natural gas. These technologies tend to have applications in the higher power ranges of stationary generation [21].

In Turkey, there was an international center to develop hydrogen energy technologies. This center was called “International Center for Hydrogen Energy Technologies (ICHET)” and it had been successfully promoting hydrogen and fuel cell technologies in Turkey. In our country, there are many applications for hydrogen. For instances, fuel cell powered forklift, UPS installations, island projects, eco-caravan that is hybrid project, hydrogen refueling station, hybrid hydrogen bus and hydrogen powered boats are ICHET projects in Turkey [25].

3. PRODUCTION OF HYDROGEN FROM HYDROCARBONS

3.1 Hydrocarbon to Hydrogen Technologies

At the present time, approximately more than 80 percent of the world energy demand is provided by fossil hydrocarbons-coal, petroleum and natural gas as sources shown in Figure 3-1. Hydrocarbons are the main source also for hydrogen production industrially. The reason of using hydrocarbon is that energy demand of process is lower than processes using other sources such as water and electrolysis.

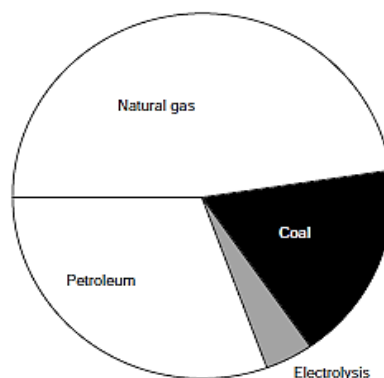


Figure 3-1 : World hydrogen production structure [20].

Therefore, the high amount of hydrogen for industrial uses is produced from natural gas, oil and coal and a smaller percentage is obtained by electrolysis of water [5]. Figure 3-2 (a) provides the comparison of the theoretical energy consumption for producing hydrogen from different hydrocarbons, coal, and water (by electrolysis). It can be seen that the production of hydrogen from light hydrocarbons requires the least amount of energy, whereas hydrogen generation by water electrolysis requires the most energy. Moreover, Figure 3-2 (b) presents a comparative assessment of the

theoretical yields of hydrogen produced by steam gasification of different hydrocarbon feed stocks and coal

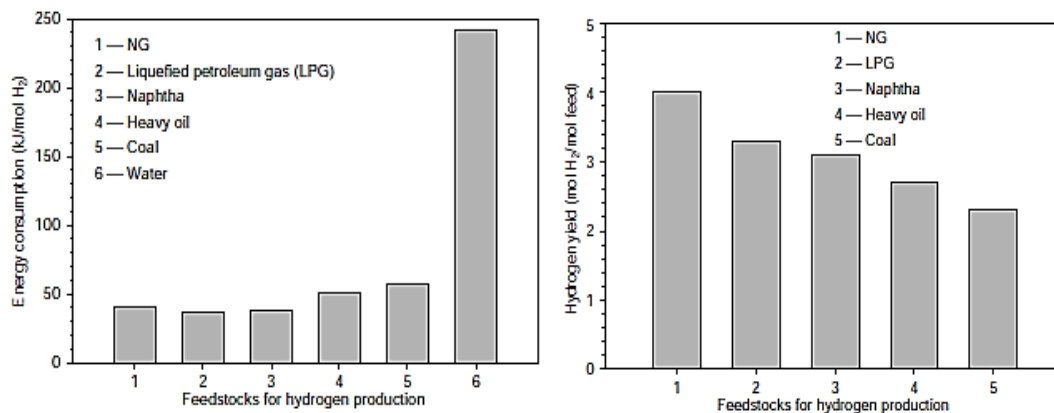


Figure 3-2 : (a) Theoretical energy consumption for hydrogen production from different feed stocks. (b) Maximum theoretical yield of hydrogen produced by steam reforming (gasification) of different feed stocks [2].

3.2 Oxidative Processing of Hydrocarbons

3.2.1 Steam reforming

Natural gas is the most attractive feed for producing hydrogen and contains approximately 90% methane. It is widely available, easy to handle and relatively cheap. Moreover, natural gas has the highest H/C ratio of all fuels and this minimize the quantity of by-product carbon dioxide. Therefore, for steam reforming, generally methane is used [26].

Steam reforming has been the most efficient, economical and widely used process for hydrogen and hydrogen/carbon monoxide production. Hydrocarbons (mainly natural gas) and steam catalytically are converted to hydrogen and carbon oxides. In addition, this reforming process releases CO₂ to the atmosphere as a byproduct. In order to eliminate environmental effect of steam reforming, CO₂ should be captured and sequestered, however, additional step cause increasing the cost of production.

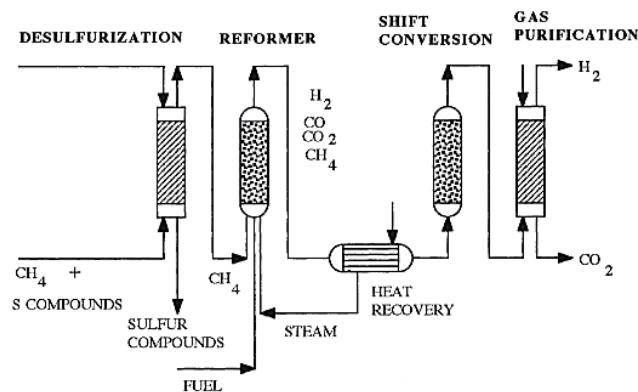


Figure 3-3 : Process flow diagram for hydrogen production by using steam-methane reforming SMR [5].

The steam-methane reforming reaction is;



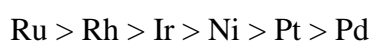
This is a highly endothermic reaction which is supported by heat from the reformer furnace. The resulting mixture is known as ‘synthesis gas’ (or ‘syngas’) and it is in fact a general term that is used to describe the combined products – hydrogen and carbon monoxide – from the gasification of any carbonaceous fuel. Therefore, the synthesis gas from the reformer is rich in H_2 and in CO . The water gas shift (WGS) reaction is described below.



It is used to increase the H_2 content [27]. It should be emphasized that CO_2 is not only produced via the shift reaction (2), but also directly via the steam reforming reaction (3). This implies that reaction (3) is not just the ‘overall reaction’, despite the fact that in literature steam-methane reforming is often considered to be a combination of reactions (1) and (2) only [28].



The development of efficient steam reforming catalysts is very active field of research because it has great importance for industrial process to produce hydrogen. For steam reforming, nickel and noble metals such as Ru, Rh, Pd, Ir, Pt are used as the active metals in catalysts. The relative catalytic activity of metals in the SM reaction is as follows:



Generally, Ni is less active than some noble metals but, it is the most widely used because of its low cost [29]. Bej et al. studied steam reforming process to produce

hydrogen by using nickel catalyst. 95.7 % methane conversion was achieved under optimum conditions [30].

3.2.2 Partial oxidation

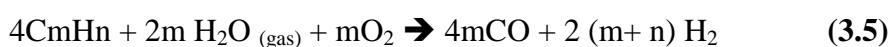
The partial oxidation (POx) of hydrocarbon is one of the major production methods for hydrogen on a commercial scale. In this process, a fuel and oxygen are combined in proportions and fuel is converted to a mixture of H₂ and CO. If methane is used as fuel;



The overall process is exothermic due to a sufficient amount of oxygen added to a reagent stream. Generally, sufficient air or oxygen is added so that the heat effects in the reactor balance out and the reaction is self-sustaining. This gives the advantage of a more compact reactor design since there is no need for a heat-exchanger. The disadvantage of employing air in partial oxidation is that the product gases are diluted by nitrogen resulting in larger WGS reactors and gas purification units. The POx process can be carried out catalytically or non-catalytically. The non-catalytic POx process operates at high temperatures (1100–1500 °C), and it can utilize any possible carbonaceous feedstock including heavy residual oils (HROs) and coal. The catalytic process is carried out at a significantly lower range of temperatures (600–900 °C) and, generally, uses light hydrocarbon fuels as a feedstock, for example, NG and naphtha [2, 26]. Wang and Ruckenstein studied on varying the cobalt loading of Co/MgO catalysts. They reported that at 1123 K, only catalysts with Co loading of 12 wt. % or greater had methane conversions of over 80% and CO and H₂ selectivity of over 90%; with a 6 wt. % Co/MgO catalyst, the methane conversion was below 20% [31].

3.2.3 Auto thermal reforming

The auto-thermal reforming process is a combination of SMR (endothermic) and POx (exothermic) technologies. A hydrocarbon feedstock (methane or a liquid fuel) is reacted with both steam and air (or oxygen) to produce a hydrogen-rich gas, i.e.,



The reaction takes place at high temperature (950-1100 °C) and at pressures up to 10MPa. The auto-thermal reformer requires no external heat source and no indirect

heat-exchangers. This is a great advantage of auto-thermal reforming, in contrast to steam reforming or partial oxidation. This feature makes it interesting for many applications, especially for smaller decentralized plants. Auto-thermal reformers typically offer higher system efficiency (80-90% is possible) than partial oxidation units. Combustion conditions have to be carefully controlled to avoid carbon formation but, overall, the unit has the advantage of being able to operate at very low steam-to-carbon ratios (as low as 0.6) [26, 32].

3.2.4 Carbon dioxide reforming of hydrocarbons

The CO₂ reforming of hydrocarbons is an alternative to SMR and POx processes, where CO₂ plays the role of an oxidant. Sometimes the process is also called stoichiometric reforming, but more often it is referred to as dry reforming. It is a highly endothermic process requiring high operational temperatures of 800–1000°C. Owing to the presence of CO₂ in the feedstock, the process produces synthesis gas with high CO/H₂ ratio (1:1). Therefore, a lot of attentions have been recently paid to the CO₂ reforming of methane to syngas. The reaction for methane is described below by eqn. (3.6):



At higher temperatures (>800°C), the carbon molar fraction in the mix drops, and the H₂ and CO molar fractions become predominant. Most of research on CO₂ reforming of methane relates to Ni-based catalysts, because Ni exhibits high catalytic activity (comparable to other noble metals) at lesser cost [2, 33].

3.2.5 Steam iron process

One of the oldest ways of producing hydrogen is the steam-iron process. This process is a coal based process; the synthesis gas generated from coal is used for the reduction of iron oxide to iron in the iron generator. Hydrogen is obtained from the reaction of steam with iron oxide. It has four main steps; 1. coal gasification, 2. Iron generation, 3. hydrogen generation and 4. Purification. This process has grown in recent times, due to its simplicity, the high purity of hydrogen obtained, which is especially important for the use of hydrogen in fuel cells, the feedstock flexibility and the possibility to use renewable energy sources in this process [5, 34].

3.2.6 Plasma reforming

There is a growing interest in electricity-assisted generation of syngas and hydrogen. In these processes, electricity alone or a mixed source of energy can be used to provide the syngas generation process with the required energy input. Use of electricity allows a better control and useful modularity of the syngas generation equipment [35]. Depending on the type of electric arc used and the chemical environment in the reformer reactor, electricity-assisted systems for hydrogen production can be categorized as follows: thermal versus non thermal plasma and oxidative versus oxidant-free plasma systems [2].

3.2.7 Photo-production of hydrogen from hydrocarbons

Photo catalytic production of hydrogen is a potentially attractive approach in converting solar photon energy to chemical energy of hydrogen. Owing to the high dissociation energy of CH₃-H bond (4.48 eV), methane absorbs irradiation in vacuum ultraviolet (UV) region. The absorption spectrum of methane is continuous in the region from 1100 to 1600 Å (absorption coefficient $k = 500/\text{atm}/\text{cm}$) [36]. Unfortunately, the wavelengths shorter than $\lambda = 160$ nm are present neither in the solar spectrum, nor in the output of most UV lamps. Therefore, the production of hydrogen and other products by direct photolysis of methane does not seem to be practical. However, the use of special photo catalysts allows activating and converting hydrocarbons to H₂ under the exposure to the wavelengths extending well into near-UV area (300–360 nm) that are present in solar spectrum (about 4–5% of the total spectrum).

3.3 Non-oxidative Processing of Hydrocarbons

3.3.1 Thermal decomposition of hydrocarbons

When hydrocarbons are heated to a high temperature, hydrocarbons are converted into hydrogen and carbon that is shown in reaction (3.7);



The amount of energy for this process depends on the nature of the hydrocarbon. The dissociation energy for C-H bond in methane is one of the highest among all organic compounds. Methane decomposition reaction is a moderately endothermic process:



The thermodynamic equilibrium data for methane decomposition reaction is shown in Figure 3-4.

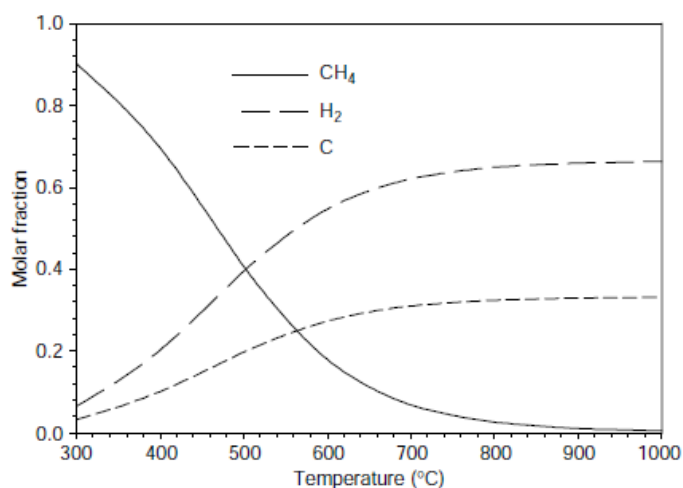


Figure 3-4 : Thermodynamic equilibrium data for methane decomposition reaction at atmospheric pressure

At temperatures above 800 °C, molar fractions of hydrogen and carbon products approach their maximum equilibrium value. The energy requirement of hydrogen produced (37.8 kJ/mole H₂) is less than that for SMR reaction (68.7 kJ/mole H₂). It is an endothermic process and less than 10 % of the heat of methane combustion is needed to drive the process. Moreover, hydrogen is produced as major product and carbon is occurred as a by-product. No CO is formed in the reaction. There is no need for WGS reaction and energy-intensive gas separation stage [2].

3.3.2 Catalytic decomposition of hydrocarbons

There have been many attempts to use catalysts to reduce the maximum temperature of methane thermal decomposition because methane decomposition reaction requires high temperatures [37]. The advantages of this process are fuel flexibility, relative simplicity and compactness, clean carbon by-product, and reduction in CO₂ and CO emissions. Various monometallic and bimetallic catalysts are investigated for the

decomposition of gaseous and liquid hydrocarbons to H₂ and carbon materials [38, 39]. Moreover, carbon based catalysts are also attractive catalysts to produce hydrogen from hydrocarbons.

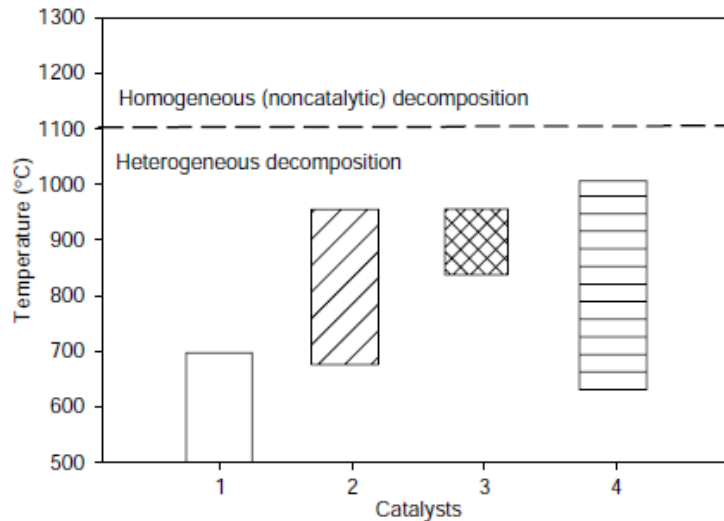


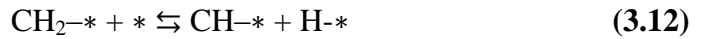
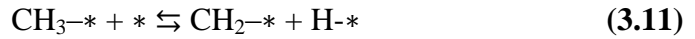
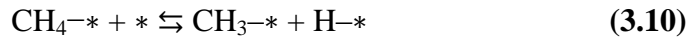
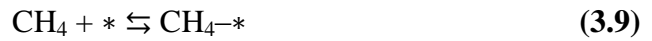
Figure 3-5 : Summary of literature data on methane decomposition catalysts and preferred temperature range; Catalysts: 1 = nickel, 2 = iron, 3 = carbon, and 4 = other transition metals (Co, Pd, Pt, Cr, Ru, Mo) [2].

Common catalysts used are mainly transition and noble metals such as Ni, Fe, Pd, Co, etc. Catalysts are supported on high surface area substrates such as Al₂O₃ and SiO₂, etc. [40]. Figure 3-5 summarizes reported literature data on different catalysts for methane decomposition and the preferred temperature range. The dotted line separates catalytic and non-catalytic temperature regimes of the methane decomposition reaction. Nickel catalysts have lower temperature for hydrocarbon decomposition than others. However, there is a catalyst deactivation problem associated with the carbon build up on the catalyst surface. Carbon is produced as a byproduct of the process and over period of time it accumulates on the catalyst surface affecting its activity and in some cases causing the reactor clogging [37]. Catalysts are not only parameter for catalytic decomposition process to produce hydrogen and valuable carbon. There are also many parameters such as heating sources, reactor types, pre-treatment methods, substrates types, reaction temperature, and catalyst preparation methods.

3.3.2.1 Literature studies

Catalytic decomposition of hydrocarbon is one of the non-oxidative processes that its aim is to produce CO_x-free hydrogen. Methane is generally preferred as hydrocarbon source. Moreover, natural gas (90% methane) is used by many researchers for its high yield hydrogen potential and economic aspects. Methane is converted into hydrogen and filamentous carbon as by-product. Surface reactions for the formation of the filamentous carbon and hydrogen by methane cracking are derived:

Surface reactions:



where“*” is an active site [41].

Various types of catalysts have been used to reduce the decomposition temperature in this process, as mentioned previously. In addition to this, catalyst function is to reduce the activation energy required for methane decomposition. There is no general agreement among researchers about the catalytic activities of metals in catalytic methane decomposition.

Koerts et al. [42] reported that the methane decomposition activity rate by the transition metals follow the order: Co, Ru, Ni, Rh > Pt, Re, Ir > Pd, Cu, Fe, Mo. However, Avdeeva et al. [43] demonstrated that iron group metals have the highest activity for hydrocarbon cracking and among these metals; nickel has higher catalytic activity than cobalt and iron. The iron group metals follow the order: Ni > Co > Fe. Nickel is particularly active for hydrocarbon cracking, especially for methane. Cobalt and iron can also be used to catalyze methane cracking but their carbon/active site capacities are much lower than that of nickel, with additional problems in the case of cobalt, which are associated with its higher cost and toxicity [44].

Parmon [45] reported the development of a Ni-based catalyst with CH₄ conversion at 60–77% and H₂ yield of 80 vol. % at 700– 800 °C in a pilot with a revolving reactor system.

Furthermore, the amount of metal in catalysts can affect hydrogen and carbon efficiency during reaction. Venugopal et al. [46] investigated the hydrogen yield effect while using various loading (5-90wt. %) of nickel silica for hydrogen production. Results revealed that increasing nickel loading has a positive effect on methane conversion and catalyst stability until 30% is reached, and there a maximum in conversion was achieved. Addition of metal to catalyst may affect reaction conditions and efficiency.

Chesnokov and Chichkan [47] studied 70%Ni-10%Cu-10% Fe/Al₂O₃ catalyst for methane cracking, and the addition of iron to catalyst. The optimal operating temperature range is increased from 600 to 675 °C for Ni/Cu/Al₂O₃ to 700-750 °C while maintaining good catalyst stability.

Shah et. al [48] evaluated bimetallic catalysts activities for hydrogen production by catalytic decomposition of methane. Binary, Fe-M (M= Pd, Mo or Ni) catalysts supported on alumina. At reaction temperatures of 700-800 °C, the product stream was achieved over 80 vol. % of hydrogen.

The catalysts include active material and the support. The support material directly affects methane conversion by affecting the surface area of metal subjected to the reaction. Pinilla et al. [49] investigated methane decomposition in a fixed-bed reactor using iron based catalysts. The effect of the textural promoter is studied. It is concluded that iron catalyst prepared with Al₂O₃ showed slightly higher catalytic performance as compared to MgO substrate.

Takenaka et al. [50] studied the decomposition of methane over supported-Ni catalysts and they compared the effects of the supports on the catalytic lifetime. Ni catalysts supported on SiO₂, TiO₂ and graphite showed high activities and long lifetimes, however the catalysts supported over Al₂O₃, MgO and SiO₂.MgO substrates were inactive for the reaction.

Particle size of catalysts is also affecting parameter on catalytic decomposition. Ahmet et al. [40] explained that the catalytic activity of the pure Ni catalysts for CH₄ decomposition was strongly related to the crystalline size of the reduced Ni. The Ni

catalyst with crystalline size of about 10.8 nm had the highest carbon and H₂ yields, and the nickel crystalline of about 20 nm gave relatively lower carbon yields. Further increasing the nickel crystalline size to about 24 nm led to extremely low catalytic activity, and an increase up to 26 nm resulted in total deactivation toward CH₄ decomposition.

Takenaka et al. [51] investigated the effect of supports on CF formation for Co-based catalysts. The 10–30 nm range for Co particles was preferred for CF formation. Ermakova et al. [52] studied about Fe/SiO₂ catalysts with different surface areas and particle sizes, and it was concluded that approximately catalysts which have 30-45 nm particle sizes gave maximum carbon yield on methane cracking.

The effect of temperature is another parameter to achieve high efficiency to produce hydrogen and carbon. Ermakova et al. [44] observed the optimum operation for nickel catalyst in the 500-552 °C temperature range. At temperatures higher than 552 °C, solid carbon is formed rapidly and causes clogging. At temperatures lower than 500 °C, carbon is formed at a rate lower than the carbon solubility in nickel, it causes reducing the driving force for carbon diffusion in the metal. Catalysts deactivates without occurring adequate carbon [53].

Daniela et al. [54] indicated that alumina supported nickel catalysts gave better result on carbon and hydrogen production at 500 °C than at 700 °C.

Amiridis et al. [53-57] studied decomposition of gaseous hydrocarbons such as CH₄ and ethane over Ni/SiO₂ catalysts in the temperature range 450–650 °C. The initial high activity of the catalyst yielded 35% CH₄ conversion at 550 °C. Fe catalysts can decompose methane at a temperature range of 700–1000 °C, but Fe catalysts have a very short lifetime.

Ammendola et al. [58] showed that catalysts containing Ni and Fe tested. It was reported that the result of having a maximum operating temperature of 550 °C for Ni-based catalysts is thermodynamically limited methane conversion at this temperature. On the other hand, Fe-based catalysts are more stable at higher temperatures (700-1000 °C), but deactivation occurs rapidly, resulting short lifetime.

Heating sources and reactor types are important factors on catalytic decomposition of methane. There are many studies on the use of an electrical furnace as a heating source for the catalytic decomposition reactor, while there are few focusing on the

use of concentrated solar energy, plasma or a molten-metal bath as alternative heating sources. Concentrated solar energy is a clean source of high temperature and heat transfer is occurred directly to reaction site, however, it is not good for hydrocarbon that absorb radiation. To solve this problem, transparent window is used [59]. Plasma is used as an environmental friendly heating source. Microwave plasma commonly used in MW ovens. The major advantage of this new process is the total conversion of hydrocarbon into hydrogen and solid carbon.

Muradov et al. [60] studied thermo catalytic decomposition of natural gas by using plasma generated carbon based catalyst. The plasma-generated carbons exhibit highest catalytic activity for natural gas decomposition among other known carbon based catalysts.

Another important factor is the type of reactor equipment used. Fixed bed and fluidized bed reactors are the most commonly used types for catalytic decomposition of methane. While using fixed bed reactor, there is a problem about carbon deposition over the external surface of the catalyst particles. For experiments conducted over a long duration, fixed bed will be gradually filled with solid carbon and finally blocking reactant gas flow [61]. However, Ashraf et al. [62] investigated that the performance of methane cracking with various type of catalysts was compared by using fixed and fluidized type of reactors. They showed that methane conversion in fixed bed reactor is higher than fluidized bed reactor as shown in Figure 3-6.

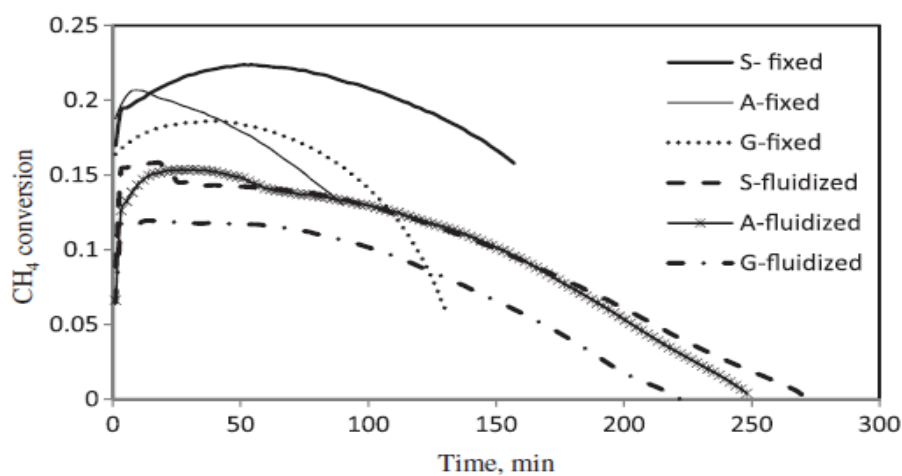


Figure 3-6 : Fixed and fluidized beds conversion at 550 °C. (G Ni/ γ Al₂O₃, A Ni/ α Al₂O₃, S Ni/SiO₂).

The lower conversion is observed in the fluidized bed because some amount of methane passes through the bed in the bubble phase and this amount increases when increasing the flow rate. However, catalysts are deactivated faster in the fixed bed than in the fluidized bed. The reason of this is explained as the accumulation of solid carbon in fixed bed reactor. It should be removed periodically.

The catalyst pre-treatment method is another important factor for performance. After preparation of catalyst, the catalyst needs to be activated. The pre-treatment includes calcination and reduction. Any residual precursor species is removed and precursor material is changed into metal oxide in calcination step. After calcination, metal oxide is converted to the active metal phase in reduction step. The temperature and the duration of pre-treatment steps influence how much catalyst is activated. Calcination or reduction above the optimum temperature also affects the catalyst texture and may cause sintering, whereas using temperatures lower than the optimum temperature may not activate the catalyst totally.

Echegoyen et al. [63] studied the effect of calcination temperature on copper doped nickel catalyst and they found that the highest yield for catalyst is achieved at the temperature of calcination 600°C.

Venugopal et al. [46] investigated the yield effect while using various loading of nickel silica for hydrogen production. It is reported that nickel oxides in the bulk and those attached to silica is reduced at 300-400°C and 400-500°C, respectively.

Owing to a high value and practical importance of carbon filaments, catalytic decomposition of methane and other hydrocarbons as a means of production of different types of filamentous carbon (carbon nanotubes [CNTs], carbon nano-fibers, etc.) has been a very active area of research for several decades. It can be produced during catalytic decomposition of methane as by-product. Carbon filaments with their mechanical and electrical properties have vital practical applications in areas such as composite materials, electronics, catalysis, space, and military. Carbon filaments of different structure produced by metal-catalyzed decomposition of methane are shown in Figure 3-7.

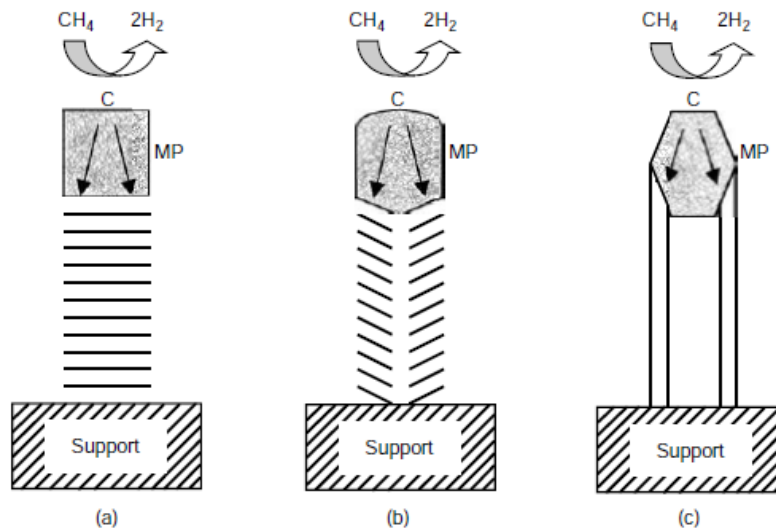


Figure 3-7 : Schematic representation of carbon filaments of different structure produced by metal-catalyzed decomposition of methane. (a) Platelet structure, (b) “herringbone” structure, and (c) ribbon structure. MP denotes a nano-sized metal particle [2].

The metal–support interactions are found to play a determinant role for the growth mechanism [64-65]. Weak interactions yield tip-growth mode whereas strong interactions lead to base-growth. Both growth modes are schematically shown in Figure 3-8.

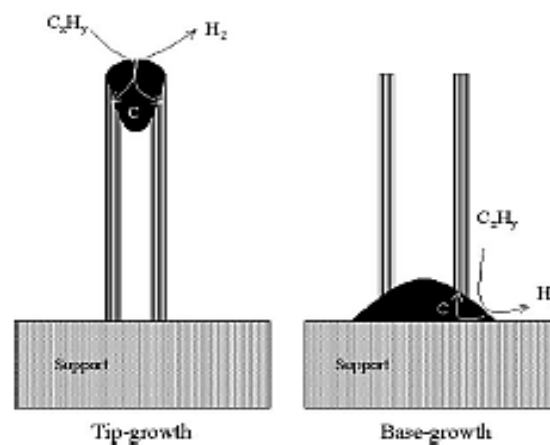


Figure 3-8 : The two growth modes of filamentous carbon.

Carbon filaments are occurred as carbon nanotubes having diameter ranging from 0.8 to 300 nm. Carbon nanotubes can be categorized into single walled carbon nanotubes (SWNTs) and multi-walled carbon nanotubes (MWNTs) depending on the number of

graphene layer. SWNTs consist of single layer graphene sheet and MWNTs consist of several layers of graphene sheets rolled into a cylinder [66].

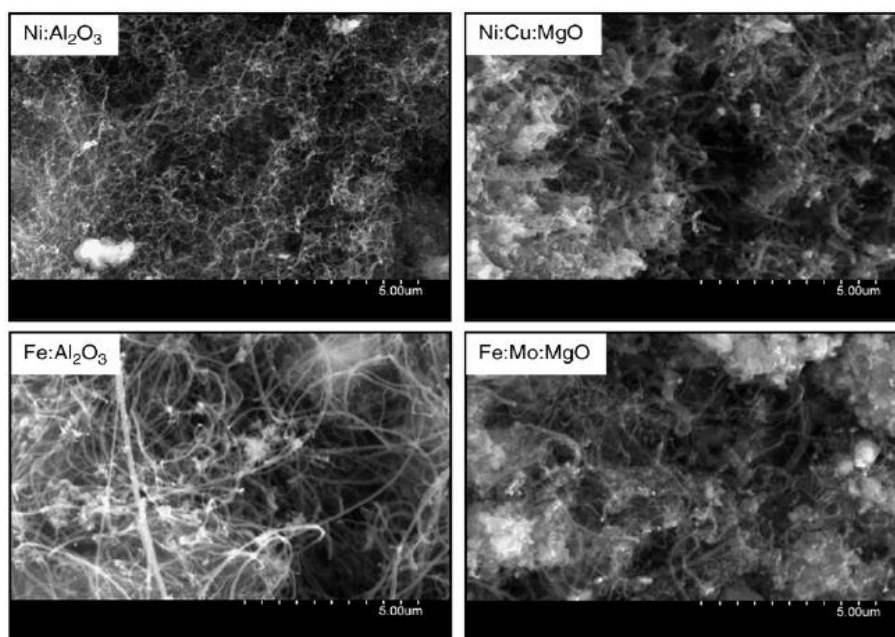


Figure 3-9 : SEM micrographs of the carbon nanostructures formed by CDM with each catalyst.

Pinilla et al. [67] evaluated that catalysts, consisting of Ni, Ni:Cu, Fe or Fe:Mo as the active phase and Al_2O_3 or MgO as a textural promoter, were tested for the catalytic decomposition of methane in a rotary bed reactor. They resulted that the Ni-based catalysts allowed the large-scale production of fishbone-like carbon nano-fibres, whereas the use of the Fe-based catalysts promoted the production of carbonaceous filaments having a high degree of structural order, consisting of both chain-like carbon nano-fibres and carbon nanotubes. SEM (Scanning Electron Microscope) and TEM (Transmitted Electron Microscope) images are shown in Figure 3-9 and Figure 3-10 respectively.

3.3.3 Plasma-assisted decomposition of hydrocarbons

Conventional catalytic technology, for small and moderate scale portable applications, has many problems because of relatively low specific productivity, high metal capacity, and equipment size. Thermal plasma, having very high energy density media, is an alternative process for hydrogen and syngas production. In this process, plasma replaces catalysis and helps to accelerate chemical reactions mainly

because of high temperature effect. Plasma chemical methods have advantages such as high specific productivity of apparatus, low investment, and operation costs. However, there is a disadvantage such as consuming high electric energy [68].

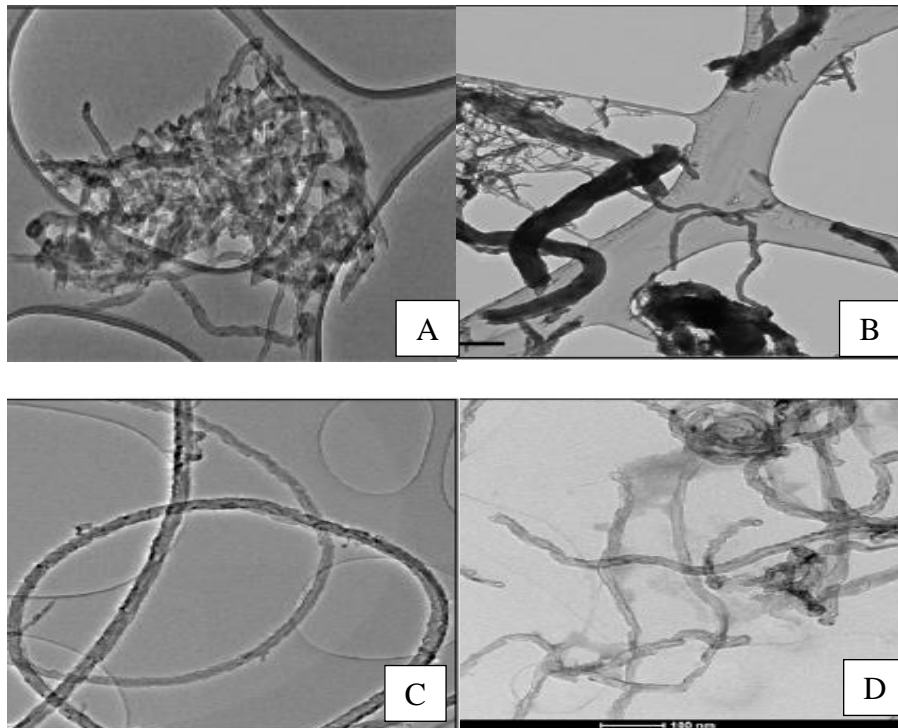


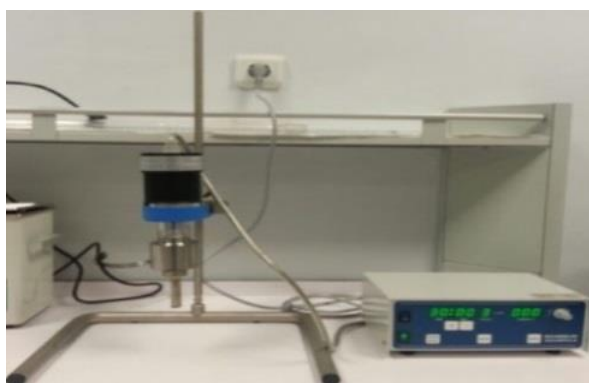
Figure 3-10 : TEM micrographs of the carbon nanostructures formed by CDM. A: Ni:Al₂O₃ catalyst. B: Ni:Cu:MgO catalyst, C: Fe:Al₂O₃ catalyst D: Fe:Mo:MgO catalyst.

For non-thermal plasma, the electrical power is low. The temperature of neutral species does not change because the temperature of electrons is very high. In this process, the aim of plasma is not to provide energy to the system but to generate radical species. The advantages of using non-thermal plasma are related to the lower temperature that will result in lower energy consumption and lower electrode erosion since the cooling of the electrodes is generally not necessary. In addition, the size and weight of the non-thermal plasma reactors are relatively low, which is very attractive for mobile applications [69].

4. EXPERIMENTAL STUDIES

4.1 Catalyst Preparation

The catalysts were prepared by impregnating MgO and SiO₂ substrates with transition metals (Fe, Ni, and Co). The process was carried on by mixing MgO or SiO₂ with Fe(NO₃)₃·9H₂O, Ni(NO₃)₂·6H₂O and Co(NO₃)₂·6H₂O in separate processes for each catalyst. The metal and substrate is mixed with weight ratio of 10:100 which was known to obtain high hydrogen production in ethanol solution by ultrasonic mixer. The amount of metal in the solution of MgO or SiO₂, ethanol and metal compound was calculated according to the molecule ratios of metals in the compound. The prepared solution was mixed for 30 minutes in “Bandelin Sonoplus” sonicator as shown in Figure 4.1 (a) then dried in oven at 80°C for 24 hours followed by calcination in air at 500 °C for 4 h. The catalyst was then grinded to avoid any agglomeration that may affect the interaction between source gas and the surface of catalyst during hydrogen production and CNT synthesis.



(a)



Figure 4-1 : (a) “Bandelin Sonoplus” sonicator (b) Catalysts during drying process.
(c) Catalysts after grinding

4.2 Catalyst Characterization

Calcinated catalysts were characterized by X-ray diffraction (XRD), Scanning Electron Microscope (SEM), and Thermogravimetric Analyzer (TGA). Powder XRD patterns of the catalyst were recorded by Rigaku D/Max-2200/PC diffractometer using nickel filtered Cu-K α ($\lambda=1.5418 \text{ \AA}$) radiation. The step scans by using step range as 0.02° were taken between the ranges of 2θ angles from 10° to 70° . The average crystallite sizes of catalysts were calculated by using the Scherrer method;

$$L = \frac{0.89 \times \lambda}{\beta \times \cos\theta} \quad (4.1)$$

where L is the average particle size, λ is the wavelength of CuK α radiation (0.154 nm), β is the half-height width of diffraction peaks, θ is the Bragg angle [1]. Morphology of catalysts was examined by a SEM (Philips XL30 SFEG) at an accelerating voltage of 15 kV. Elemental compositions of the catalysts were determined by scanning electron microscopy coupled with energy-dispersive X-ray spectroscopy (EDX). Thermo-gravimetric analysis was performed using TGA 4000 at a heating rate of $10^\circ\text{C}/\text{min}$, ranging from 30 to 800°C under oxygen flow with rate of $20\text{L}/\text{min}$.

4.3 Hydrogen and Carbon Nanotubes Production

Hydrogen and carbon nanotubes production experiments were carried out at 500°C, 550°C and 600°C for Ni, Fe and Co at atmospheric pressure in a fixed-bed vertical stainless steel reactor having 6 mm diameter and 42 cm length. The schematic view of hydrogen production system is shown in Figure 4-2. Nitrogen (N₂) was used as carrier gas and CH₄ was used as hydrocarbon source. 0.2 gram catalyst was put into reactor for all catalysts. Electrical furnace that have 45 cm length and 12 mm inner diameter to place reactor and reactor are shown in Figure 4-3 (a). The catalyst bed temperature was also measured with a K-type thermocouple. Before the reaction, nickel, iron, cobalt catalysts were reduced at 400°C respectively with same H₂:N₂ (50:50) ratio for 2 h. The reactant gas mixture that includes methane (CH₄) and nitrogen (N₂) was fed to reactor with the flow rate 50 ml/min at various temperatures for each catalyst. The catalytic decomposition of methane was performed with CH₄:N₂ (80:20) ratio by using mass flow meter “Brooks” as shown in Figure 4-3 (b) for 3 h. The products of the reaction were analyzed by the gas chromatograph (Agilent Technologies, 7890A) as shown in Figure 4-3 (c) that was connected to the outlet of the reactor.

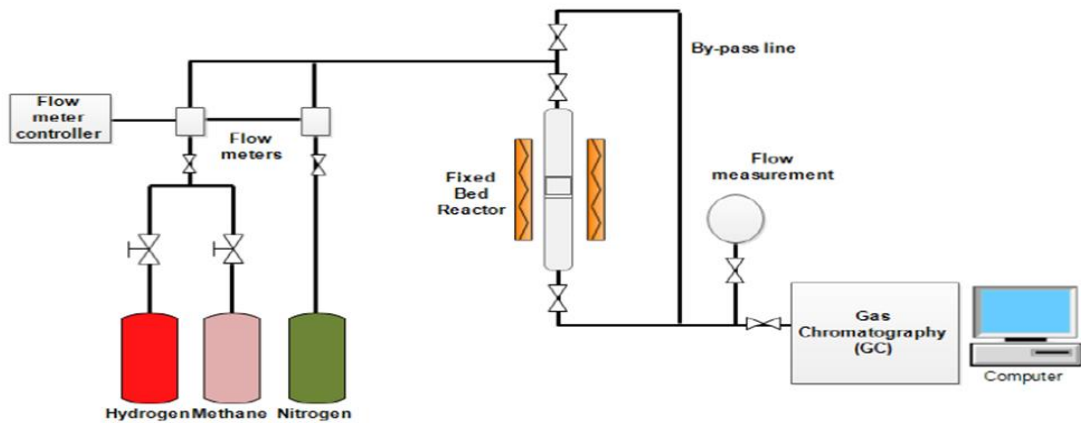


Figure 4-2 : Schematic Diagram of Hydrogen Production System



(a)



(b)



(c)

Figure 4-3 : (a) Reactor system (b) Mass flow meter (c) Gas chromatography

5. RESULTS AND DISCUSSIONS

The catalytic decomposition of methane was investigated through a fixed-bed vertical stainless steel reactor using different catalyst (Fe, Ni and Co), support materials (MgO and SiO₂) and different conditions.

5.1 Catalyst Characterizations and Hydrogen Production Results

The catalytic decomposition of methane experiments were performed in the fixed bed reactor under similar conditions in order to sought catalytic activities over different supports (SiO₂ and MgO) and different metals Ni, Fe and Co metals. The metal and substrate weight ratio was selected as 10:100 by considering the results of the previous studies on catalysts that were prepared at ITU Energy Institute laboratory [75]. Moreover, it is known that catalytic performance of the catalysts for methane decomposition strongly depends on their crystallite sizes which obtained from the XRD results. Therefore, the average crystallite sizes of prepared catalysts were calculated by using the Scherrer formula:

$$L = \frac{0.89 \times \lambda}{\beta \times \cos\theta} \quad (5.1)$$

where L is the average particle size, λ is the wavelength of CuK α radiation (0.154 nm), β is the half-height width of diffraction peaks, θ is the Bragg angle.

Methane conversions and hydrogen productions were also determined for each catalyst from the gas chromatograph data. Product gases are hydrogen, methane and nitrogen. These gases were analyzed from the peaks of the related gases that ascertained by FID, TCD1 and TCD3 detectors on gas chromatography. Percentages of product gases were determined by using an empirical formula by the areas under

the peaks. All data were recorded during 3 h of reaction time. Methane conversions (%) were calculated by the formula;

$$\text{Methane conversion}(\%) = \frac{\text{Inlet } CH_4 \text{ mole} - \text{Outlet } CH_4 \text{ mole}}{\text{Inlet } CH_4 \text{ mole}} \times 100 \quad (5.2)$$

5.1.1 Nickel catalysts

Nickel catalysts were prepared with two different support materials (SiO₂ and MgO) to investigate hydrogen production efficiency. XRD patterns of Ni/SiO₂ and Ni/MgO catalysts calcinated at 500°C for 4 h in air were given in Figure 5-1.

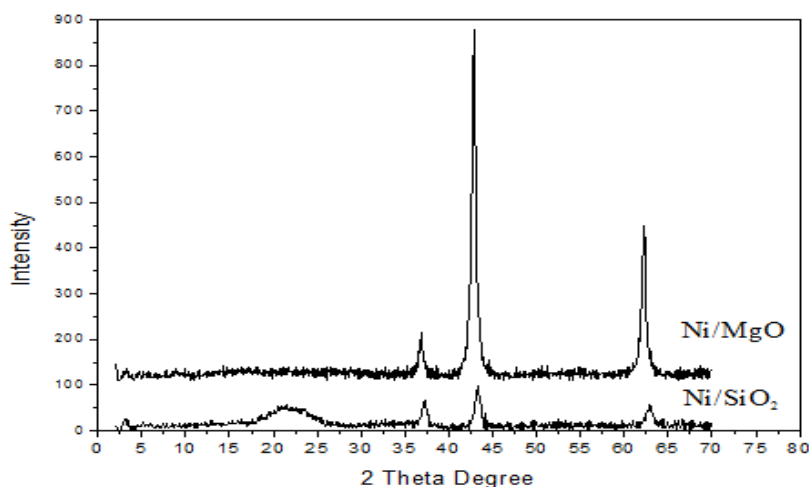


Figure 5-1 : XRD patterns of Nickel catalysts after calcination process

It conforms the reflections at $2\theta = 37.181^\circ, 43.261^\circ, 62.841^\circ$ are attributed due to the NiO phase for Ni/SiO₂ catalyst. Moreover, Ni particle size of Ni/SiO₂ catalyst is about 11.5 nm that is obtained from XRD results. For Ni/MgO catalyst, three diffraction peaks are clearly observed. The reflections at $2\theta = 36.879^\circ, 42.860^\circ, 62.240^\circ$ are related to NiO phase of catalyst and Ni particle size was calculated as 17.9 nm. There is no dramatic difference in XRD patterns between Ni/SiO₂ and Ni/MgO catalysts, but their catalytic activities are different because of their crystallite sizes. A similar result was reported in the literature [61]. In the study, Ahmet et al. demonstrated that Ni catalysts with crystalline size about 10-12 nm had the highest carbon and H₂ yields. In addition, they emphasized that the nickel crystalline size about 20 nm gave relatively lower carbon yields. Furthermore increasing the nickel crystalline size to about 24 nm gave extremely low catalytic activity, and an increase up to 26 nm resulted in total deactivation toward CH₄ decomposition [61].

Figure 5-2 (a) and Figure 5-2 (b) show the SEM micrographs and EDX analysis of fresh catalysts of Ni/SiO₂ and Ni/MgO. SEM images of the fresh catalysts exhibit the uniform diameter which shows consistent distribution of metal oxides on the surface of the support materials. EDX analyses also indicated that nickel amounts in catalysts were 11.6% and 9.7% by weight for Ni/SiO₂ and Ni/MgO respectively.

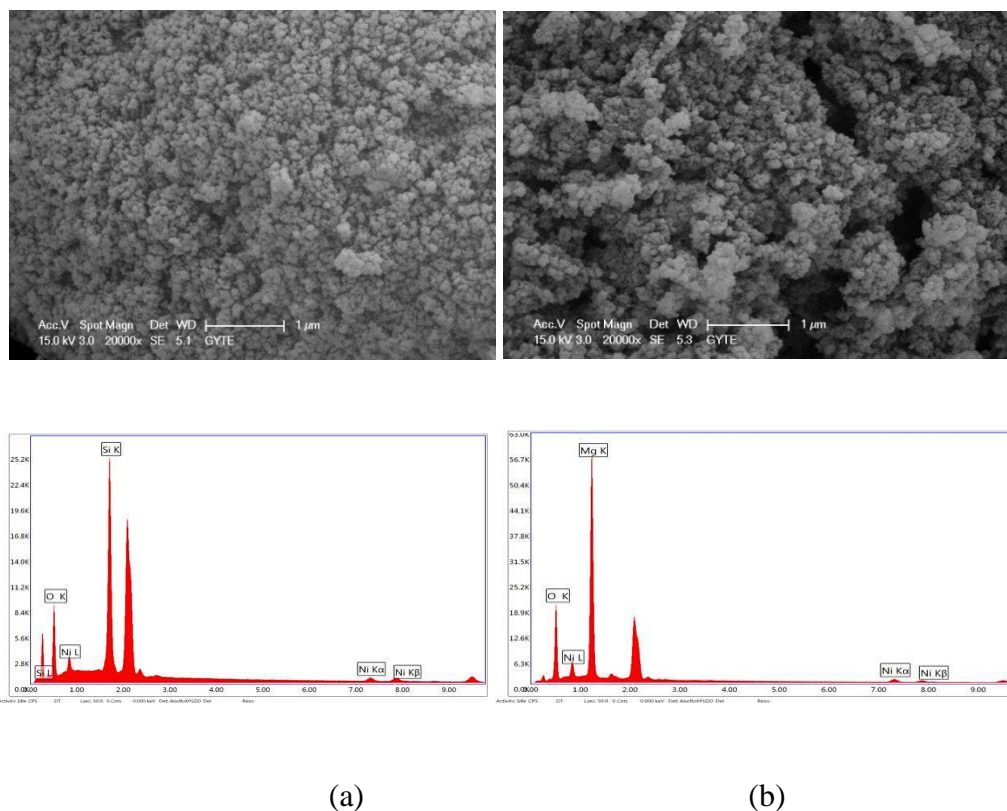


Figure 5-2 : SEM-EDX images of Ni catalyst (a) Ni/SiO₂ (b) Ni/MgO.

In catalyst preparation experiments, nickel catalysts were reduced in hydrogen atmosphere at 400°C. Similar studies [46, 72] were carried out at same reduction temperature in the literature because of high hydrogen consumption at that temperature. Tapia-Prada et al. [72] investigated the synthesis and characterization of Ni/SiO₂, Ni/Ce–SiO₂ and Co/Ce–TiO₂ catalysts and several techniques such as XRD, H₂-TPR, SEM/EDS and HRTEM. High H₂ consumption was achieved at 400°C from H₂-TPR results. A. Venugopal et al. [46] studied about hydrogen production by catalytic decomposition of methane over silica supported nickel catalyst. It has been reported that the nickel oxides is reduced at 400°C.

5.1.2 Iron catalysts

Iron catalysts were prepared with two different support materials (SiO_2 and MgO) to investigate hydrogen production efficiency. XRD patterns of Fe/SiO_2 and Fe/MgO catalysts were given in Figure 5-3.

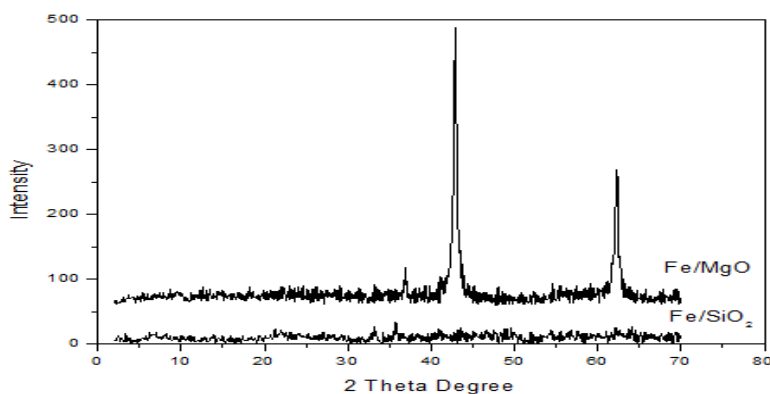
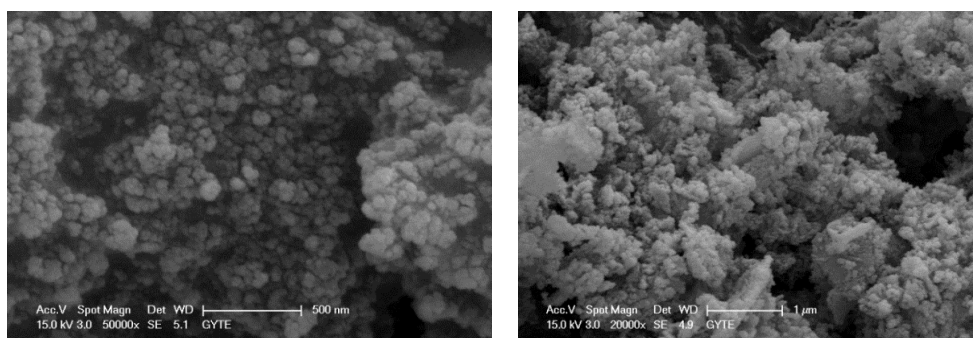


Figure 5-3 : XRD patterns of Fe catalysts

It conforms that the reflections at $2\theta = 33.21^\circ$, 35.832° are attributed due to the Fe_2O_3 phase for Fe/SiO_2 . Average particle size is between 35-40 nm for Fe/SiO_2 . For Fe/MgO catalyst, three diffraction peaks are clearly observed. The reflections at $2\theta = 36.921^\circ$, 42.92° , 62.28° are related to iron oxide phase of catalyst. These peaks indicate that $\text{Fe}(\text{NO}_3)_3$ form is converted to form iron oxide after calcination process. Moreover, particle size is calculated as 35-40 nm for Fe/MgO . This finding is in agreement with Ermakova [52] findings. They studied about Fe/SiO_2 catalysts with different surface areas and particle sizes. It was concluded that catalysts having approximately 30-45 nm particle sizes gave maximum carbon yield on methane cracking.



(a)

(b)

Figure 5-4 : SEM images of Fe catalysts (a) Fe/SiO_2 (b) Fe/MgO .

Figure 5-4 (a) and (b) display the SEM micrographs of fresh catalysts of Fe/SiO₂ and Fe/MgO. SEM images of the fresh catalysts show distribution of metal oxides on the surface of the support materials. EDX analyses also indicated that iron amounts in catalysts were 9.2% and 11.9% by weight for Fe/SiO₂ and Fe/MgO respectively.

5.1.3 Cobalt catalysts

Cobalt catalysts were prepared with two different support materials (SiO₂ and MgO) to investigate hydrogen production efficiency. XRD patterns of Co/SiO₂ and Co/MgO catalysts were given in Figure 5-5.

The reflections at $2\theta = 18.171^\circ$, 36.959° , 37.181° , 42.92° are related to cobalt oxide for both of catalysts. In addition, particle sizes of the catalysts were determined between 10-20 nm. There is no dramatic difference in XRD patterns between Co/SiO₂ and Co/MgO catalysts, but their catalytic activities are different due to their crystallite sizes. A similar result was reported in the literature [51, 71 and 74]. Nan Li et al. studied about cobalt catalyst effect on carbon nanotube synthesis. Particle size of cobalt catalysts was found as 12.8 nm [74]. Takenaka et al. [51, 71] also reported that the 10–30 nm range for Co particles was preferred for carbon fiber formation.

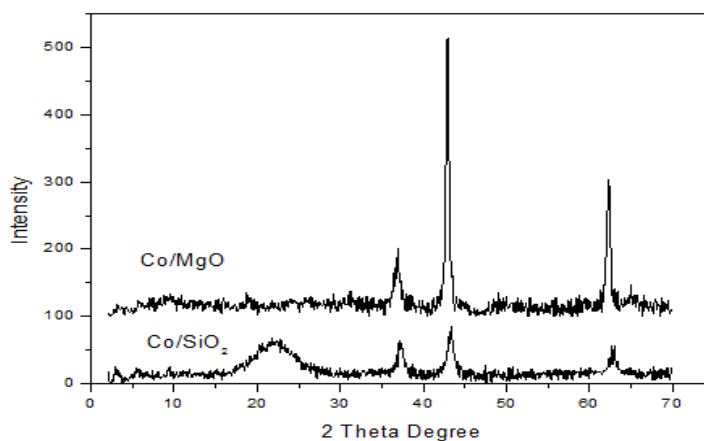


Figure 5-5 : XRD patterns of Co catalysts

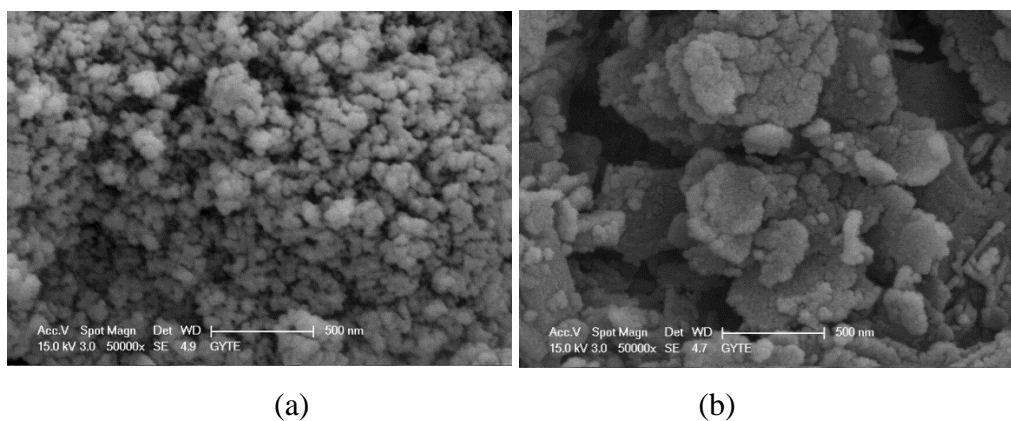


Figure 5-6: SEM images of Co catalysts (a) Co/SiO₂ (b) Co/MgO

SEM images of cobalt catalysts calcinated at 500 °C in 4h are shown in Figure 5-6. It is seen from this figure that silica supported cobalt catalyst has uniform distribution, while MgO supported cobalt catalyst has some cavities and it shows non-uniform distribution of catalyst. EDX analyses also indicated that cobalt amounts in catalysts were 8.2% and 10.9% by weight for Co/SiO₂ and Co/MgO respectively.

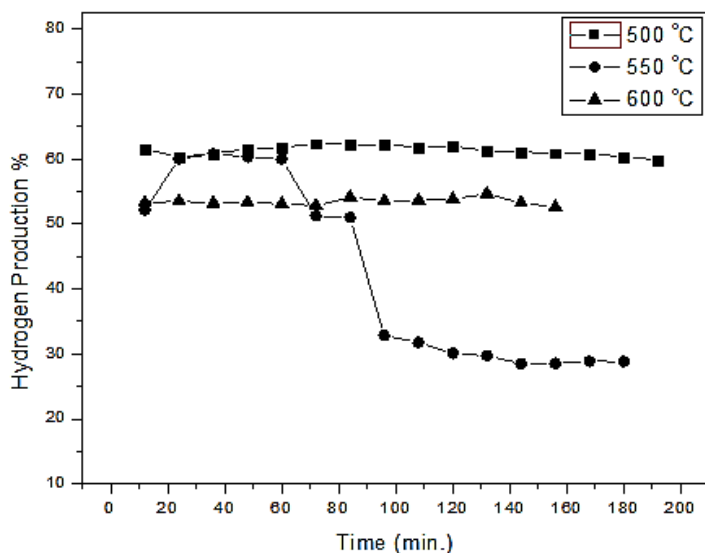
5.2 The Effect of Reaction Temperature on Catalytic Decomposition of Methane

The reaction temperature is one of the most important parameters influencing the catalyst activity, catalyst lifetime and morphology of carbon nanotubes produced. It is well known that different types of catalysts active at different reaction temperatures.

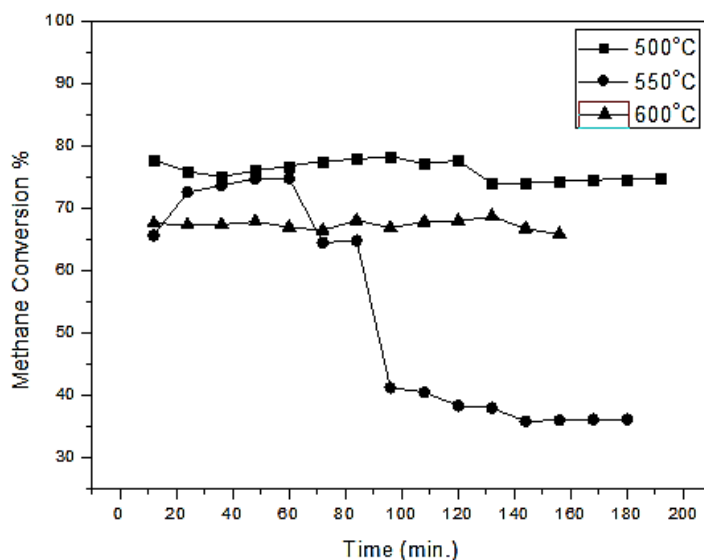
5.2.1 Nickel catalysts

In order to observe the effect of temperature for hydrogen production efficiencies and methane conversions, the experiments were performed at 500, 550 and 600°C for nickel catalysts prepared with SiO₂ and MgO during the reaction time of 3h. Hydrogen production and methane conversions efficiencies for Ni/SiO₂ and Ni/MgO catalysts at different temperatures are given in Figure 5.7 and Figure 5.8. The effect of temperature is one of parameters to achieve high efficiency to produce hydrogen and carbon. Ashraf et al. [62] studied about the effect of temperature on methane cracking by using different supported nickel catalysts. The results indicated that as

the temperature is increased higher methane conversion is achieved for all particle sizes and methane concentrations. However, Ermakova et al. [44] observed that the optimum operation temperature range was found between 500-552°C. Hydrogen productions efficiencies were achieved as 62%, 60% and 54% at 500, 550 and 600°C respectively. Moreover, initially methane conversions were also found as 78%, 67% and 65% at 500, 550 and 600°C respectively.



(a)



(b)

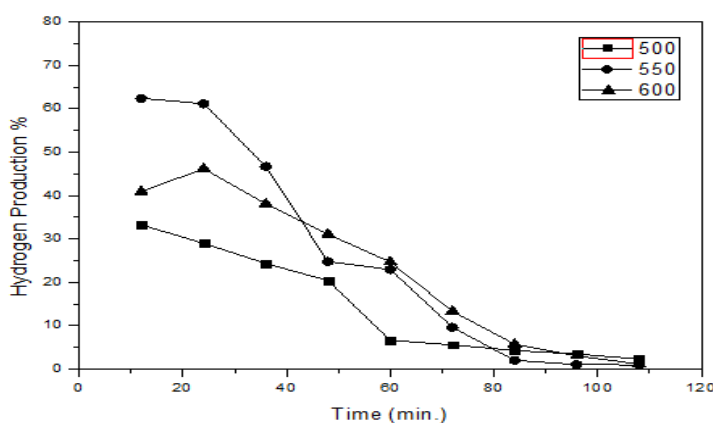
Figure 5-7 : (a) Hydrogen production efficiency (%) (b) Methane conversion (%) for Ni/SiO₂ catalyst at the reaction time of 3 h.

The main problem in catalytic methane cracking process is catalysts deactivation, since carbon is deposited on the catalyst. Carbon blocks methane access to active sites. Zhang et al. [53] studied about hydrogen production via the direct cracking of methane over 16.8wt.% nickel silica catalyst at 550°C and it was concluded that initial methane conversion was 35%. After 190 minutes, nickel catalyst was deactivated. However, in this study initial methane conversion was found higher than Zhang et al. study. Furthermore, after 3h of reaction time, there was a sharp decrease in hydrogen production and methane conversion at 550°C due to clogging. Carbon may deposit on the surface of catalyst to cover the active sites or accumulate at the entrance of the pores to block further access of the reactants to the pore mouth plugging. It is seen from Figure 5.7 that Nickel silica catalysts were more stable at the temperatures of 500 and 600°C than the temperature of 550°C. Saraswat et al. [73] investigated the effect of various metal loading and different temperatures for hydrogen production with using nickel silica catalysts. It was concluded that methane conversions were found as 17% and 30% at the temperatures of 550°C at 600°C, respectively. During the reaction time of 3h, there was no sharp decrease over hydrogen productions and methane conversions. It indicates that the clogging was not occurred during this reaction period.

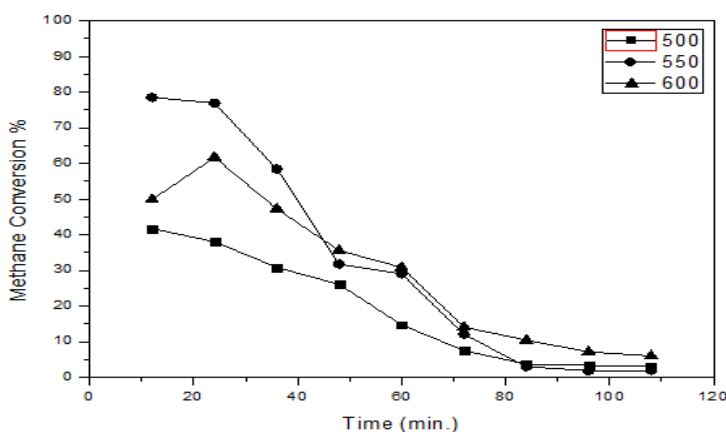
Hydrogen production efficiencies and methane conversions for Ni/MgO catalysts at different temperatures are shown in Figure 5.8. All catalysts were prepared with similar conditions. Reduction, one of the pre-treatment methods, was applied to Ni/MgO catalysts at 400°C. W. Gac et al. [77] studied about methane decomposition using nickel alumina catalysts modified with MgO. This study showed that the maximum hydrogen consumption was occurred at the temperature of 700°C. However, small peaks were obtained at the temperature of 400°C in TPR analyses. Such peaks are usually ascribed to reduction of the nickel oxide species weakly interacting with support. Further increase of the MgO content decreases reducibility. Therefore, NiO may not be converted to active Ni metal particles for hydrogen production.

Maximum hydrogen productions were achieved as 34%, 63% and 41% at the temperatures of 500, 550 and 600°C, respectively. Moreover, initially methane conversions were found as 41%, 78% and 50% at the temperatures of 500, 550 and 600°C, respectively. J.L. Pinilla et al. [67] investigated the hydrogen and carbon

nano-filament production using Fe and Ni based catalysts. Initial hydrogen production was recorded as 75 % for MgO supported Cu doped Ni catalyst at the reaction temperature of 700°C. Furthermore, H. S. Zein and A. R. Mohamed [78] researched the hydrogen production using Cu doped Ni/MgO catalyst at the temperature of 725°C. They indicated that initial hydrogen production was about 52% in first five minutes. After the reaction time of 1h, hydrogen production decreased to 16%. This result is in agreement with our experimental results and Takena study [50]. It is clear from Figure 5.8 that, after the reaction time of 1h, hydrogen production efficiency decreased to 8%, 25% and 27% at 500, 550 and 600°C respectively. Moreover, methane conversion was decreased during reaction time. Takenaka et al. [50] also studied MgO supported Ni based catalyst and they pointed out that Ni/MgO had really low methane conversion at the temperature of 500°C.



(a)

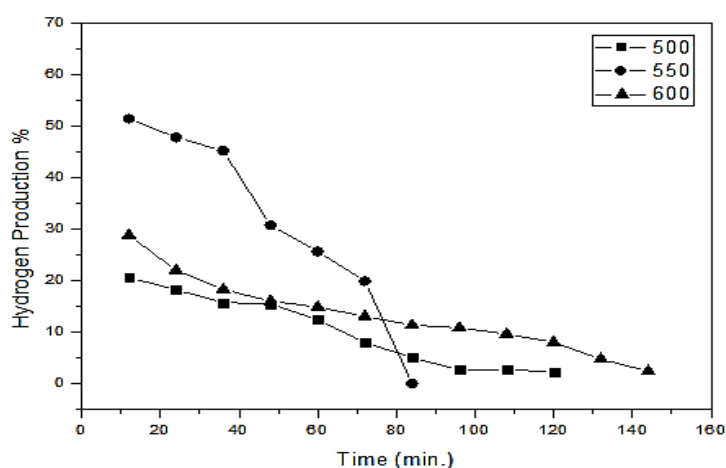


(b)

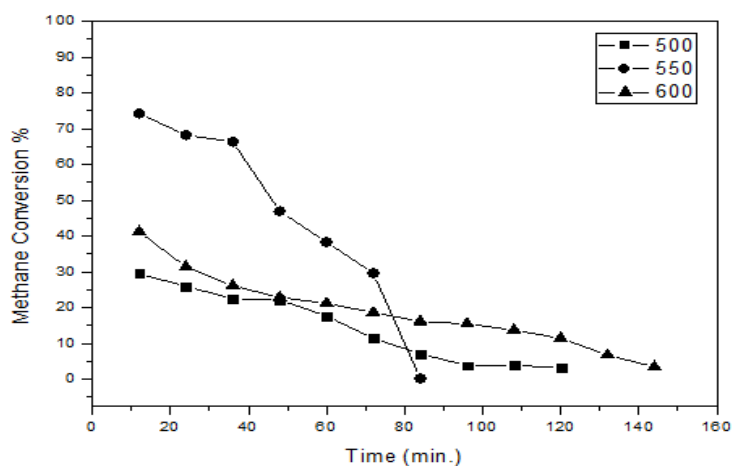
Figure 5-8 : (a) Hydrogen production efficiency (%) (b) Methane conversion (%) for Ni/MgO catalyst at the reaction time of 3 h.

5.2.2 Cobalt catalysts

In order to observe the effect of temperature on hydrogen production efficiency and methane conversion, the experiments were performed at 500, 550 and 600°C for cobalt catalysts prepared with SiO₂ and MgO during the reaction time of 3h. Before catalytic methane decomposition, cobalt catalysts were reduced with hydrogen at 400°C for 2 h. Hydrogen production and methane conversions efficiencies for Co/SiO₂ catalysts at different temperatures are given in Figure 5.9.



(a)

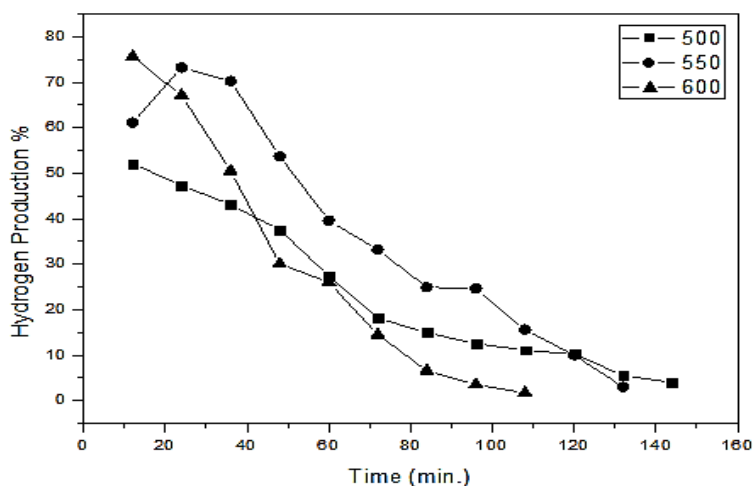


(b)

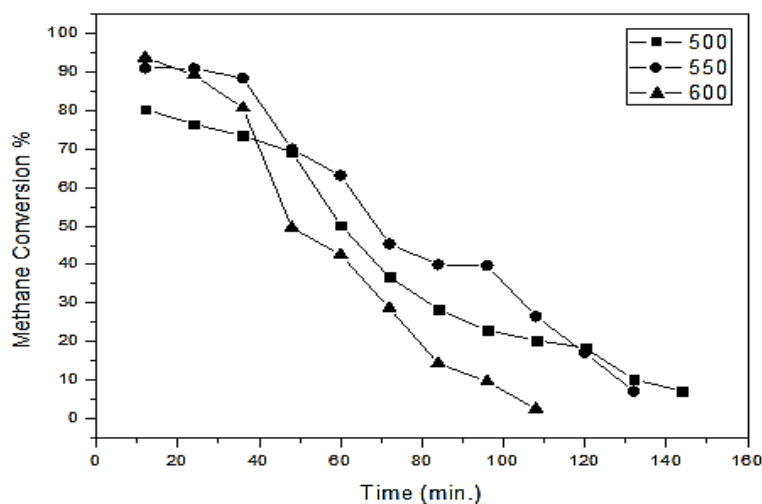
Figure 5-9: (a) Hydrogen production efficiency (%) (b) Methane conversion (%) for Co/SiO₂ at the reaction time of 3 h.

There are some studies in the literature for hydrogen production using cobalt catalyst [71, 76, 79]. Jana et al. [79] investigated that the variety of unsupported cobalt catalysts was synthesized using the Pechini method and tested for CO₂-free H₂

production via methane decomposition. It was concluded that catalyst reduction temperature should be between 300-400°C in order to achieve high hydrogen yield. However, in principle, the reducibility of cobalt is known to be affected by many factors. There is no complete reduction below 700°C. Therefore, in this study, selected reduction temperature (400°C) could not be enough for reduce cobalt oxides to cobalt metals.



(a)



(b)

Figure 5-10 : (a) Hydrogen production efficiency (%) (b) Methane conversion (%) for Co/MgO at the reaction time of 3 h.

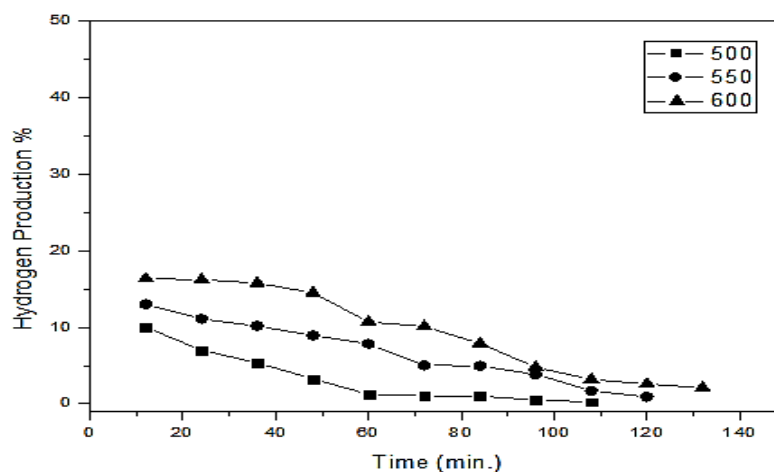
Ahmed et al. [71] summarized the hydrogen technologies produced from the hydrocarbons. They emphasized that the catalytic decomposition temperature range for Co metal catalyst should be between 650-1050°C. However, in this study, low

temperatures (500, 550 and 600°C) were selected to observe catalytic activities of catalysts. Avdeeva et al. [76] also studied about cobalt catalysts for methane decomposition reaction at 475-600°C. It was concluded that methane conversion increased with temperature while carbon formed and catalyst lifetime decreased. Moreover, methane conversion and lifetime of catalyst were inversely proportional to each other. Methane conversion was achieved as 5% during 18.5 h at 425°C. In addition to this, methane conversion was obtained as 17% during 3.5 h at 600°C. In this study, initially methane conversions for Co/SiO₂ catalyst were 30, 75 and 42% at 500, 550 and 600°C respectively. Cobalt silica catalysts were deactivated within 120, 85 and 150 minutes at 500, 550 and 600°C respectively. For 500 and 550°C reaction temperatures, methane conversions were increased while lifetimes of catalysts were decreased. However, methane conversion of cobalt silica catalyst at 600°C was higher than the methane conversion of cobalt silica catalyst at 500°C. Moreover, the catalysts at 600°C had long lifetime according to cobalt silica at 500°C. The differences between methane conversions were not so high. Therefore, the reason of this could be come from fluctuation of measurements.

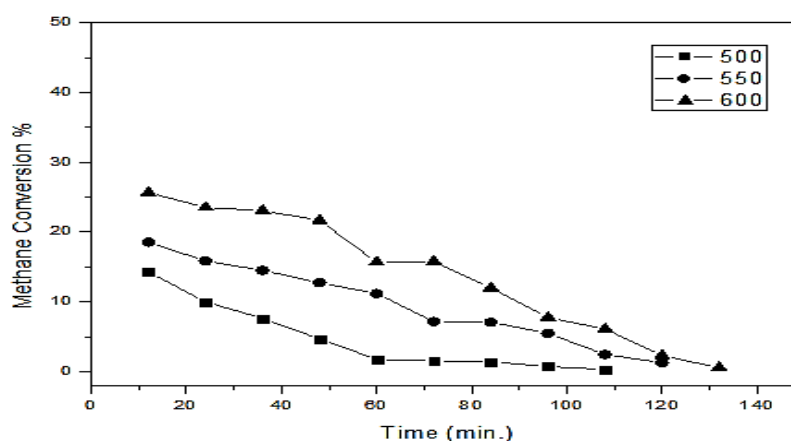
Hydrogen production and methane conversions efficiencies for Co/MgO catalysts at different temperatures are also given in Figure 5.10. Initially methane conversions were found as 80, 90 and 92% at 500, 550 and 600°C respectively. Cobalt magnesium catalysts were also deactivated within 150, 132 and 110 minutes at 500, 550 and 600°C, respectively. It was concluded that methane conversion increased with temperature while catalyst lifetime decreased for Co/MgO catalysts. Similar literature study was performed by Takenaka et al. [51]. They investigated the catalytic performance of Co catalysts supported on different supports (SiO₂ and MgO) for the formation of carbon nanofibers through methane decomposition. These experiments were performed at the temperature of 500°C. It was concluded that methane conversions were found as 35 and 70% for Co/SiO₂ and Co/MgO catalysts, respectively. Moreover, lifetimes of catalysts were 55 min and 250 min for Co/SiO₂ and Co/MgO catalysts respectively. If the results of this study were compared with Takenaka's results, methane conversion of the Co/MgO catalyst was higher (80 %) than their results (70 %) at the temperature of 500°C. On the contrary, cobalt silica catalyst had similar result with Takenaka's findings which given low methane conversions (~30%).

5.2.3 Iron catalysts

Iron-based catalysts are generally efficient at higher temperature range (700-950°C) for hydrocarbon decomposition. In order to observe the effect of lower and high temperature on hydrogen production efficiency and methane conversion, the experiments were performed at 500, 550, 600 and 800°C for iron catalysts prepared with SiO₂ and MgO during the reaction time of 3h. Before catalytic methane decomposition, iron catalysts were reduced with hydrogen at the temperatures of 400 and 700°C for 2 h. Hydrogen production and methane conversions efficiencies for Fe/SiO₂ catalysts at different decomposition and reduction temperatures are given in Figures 5.11 and 5.13.



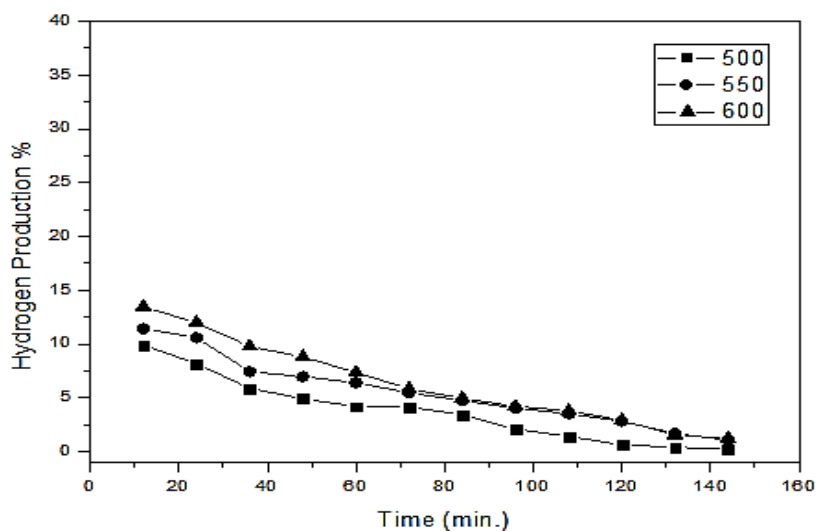
(a)



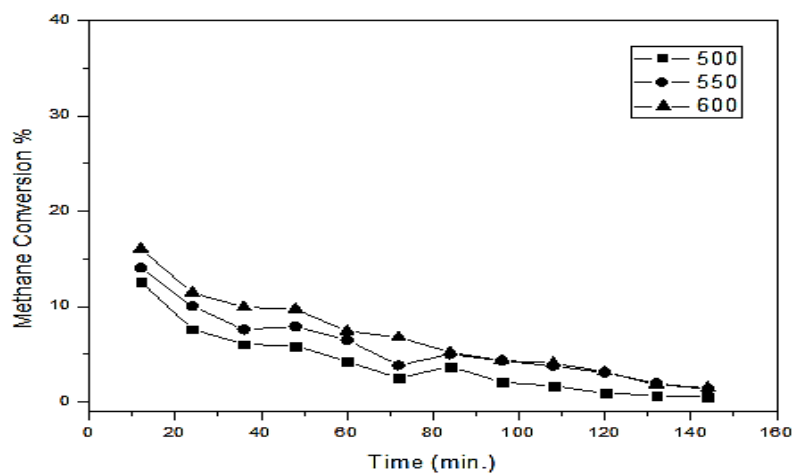
(b)

Figure 5-11: (a) Hydrogen production efficiency (%) (b) Methane conversion (%) for Fe/SiO₂ at the reaction time of 3 h.

High reduction temperature also led to high methane conversion. Calcinated iron catalyst was converted firstly from Fe_2O_3 to Fe_3O_4 formation. Finally, it was reduced to iron metals under hydrogen atmosphere at 700°C . Reduction of iron catalyst was not completely occurred at lower temperature (400°C), therefore, lower methane conversions were achieved. The reason for that could be explained the iron in metal form was more active than iron oxide form for catalytic decomposition of hydrocarbons. These findings are agreements with Ermakova's findings. Ermakova et al.[52] investigated the Ni/SiO_2 and Fe/SiO_2 catalysts for production of hydrogen and filamentous carbon via methane decomposition. It was concluded that there are two peaks of hydrogen consumption in the TPR profile of the unsupported oxide. The first one is attributed to the $\text{Fe}_2\text{O}_3 \rightarrow \text{Fe}_3\text{O}_4$ transition, and the second to complete reduction of iron oxides to Fe in accordance with literature data. Introduction of silica results in a pronounced shift of completion of the reduction towards the range of higher temperatures as 700°C . Iron oxides are known to be inclined to strong interactions with SiO_2 . An increase in the silica proportion in the catalyst results in separation of the stages of oxide species reduction. Therefore, the reason to obtain low catalytic activity could be reduction temperature.



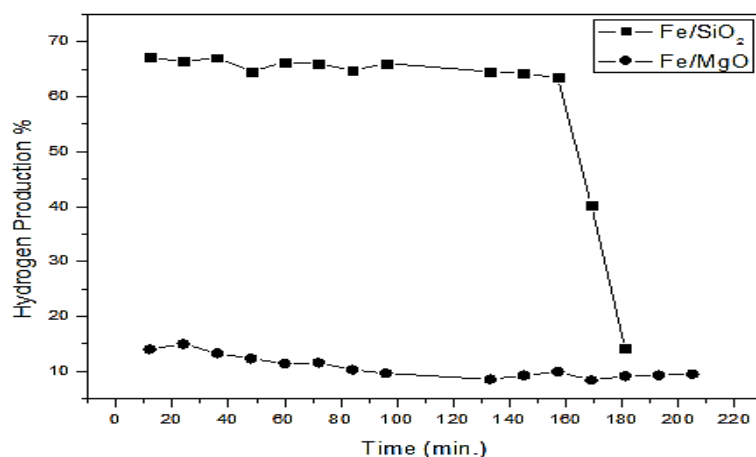
(a)



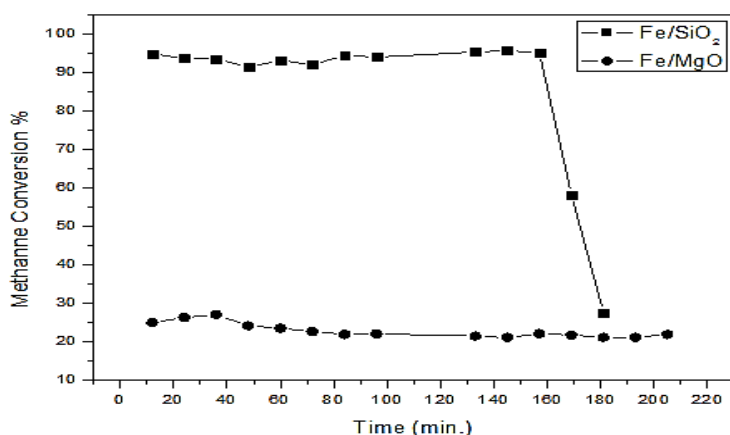
(b)

Figure 5-12: (a) Hydrogen production efficiency (%) (b) Methane conversion (%) for Fe/MgO at the reaction time of 3 h.

Hydrogen production and methane conversions efficiencies for Fe/MgO catalysts at different temperatures are also given in Figure 5.12. Initially methane conversions were found as 13, 14, 16 and 27 % at 500, 550, 600 and 800°C, respectively. By comparing with Fe/SiO₂ results low methane conversions were achieved. To improve the conversion efficiency, Fe catalysts doped with other metals (Cu, Mo, etc.) could be more active for hydrocarbon decomposition. The effect of metal doped to catalyst was investigated by Pinilla et al. in the literature [49]. They studied the catalysts, consisting of Ni, Ni:Cu, Fe and Fe:Mo with Al₂O₃ and MgO support materials for methane decomposition. Fe/MgO catalyst doped with Mo had initial methane conversion as 90% at 800°C. Therefore, the effect of metal doped Fe/MgO catalyst would be investigated for future work of this thesis.



(a)



(b)

Figure 5-13: (a) Hydrogen production efficiency (%) (b) Methane conversion (%) for Fe/SiO₂ and Fe/MgO at 800°C and the reaction time of 3 h.

Figure 5.13 present that maximum methane conversion for Fe/SiO₂ catalyst was about 95% and it stabilized between 90%-95% during the reaction time of 2h. In addition to this, it decreased suddenly to 27% at the end of reaction time. A possible explanation for this might be that of the deactivation of catalyst. However, maximum methane conversion of Fe/MgO was about 27% and it decreased to minimum 21% at the end of reaction time. This result may be explained by the fact that carbon diffuses through iron to form carbon filaments or encapsulates the active sites and blocks methane access to active sites.

5.3 The Effect of Catalysts Type on Catalytic Decomposition of Methane

The effect of catalysts type on decomposition of methane was investigated by using transition metals (Fe, Co, Ni) that extensively used in literature and the results obtained at different reaction temperatures (500, 550 and 600 °C) were presented in Figures 5.14-5.16.

The hydrogen production efficiencies of silica supported catalysts at the temperature of 550 and 600 °C were given in Figure.5.14 and 5.15. It is seen from these figures that nickel showed higher catalytic activity than other metals. The order of hydrogen production efficiencies of the catalysts is Ni>Co>Fe. Methane conversions of the catalysts had identical behavior with hydrogen production efficiencies. Similar results were reported on the other study in literature [66].

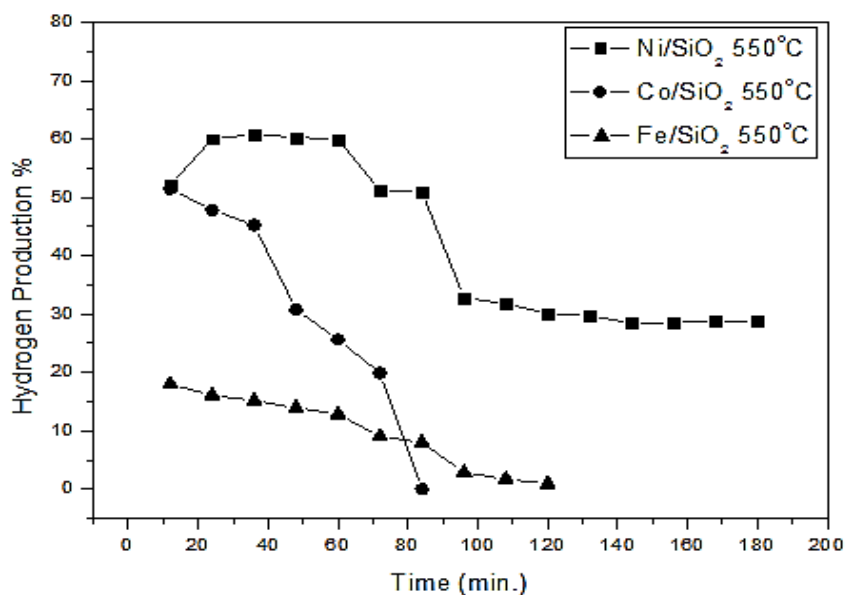


Figure 5-14: Hydrogen production efficiencies for all catalysts at 550°C

Chai et al. [66] studied on carbon nanotubes production via catalytic methane decomposition. It was concluded that supported nickel was the most effective catalyst at lower temperatures (450°C-550°C). It is well known that cobalt catalysts are hardly used due to their lower activity and lower carbon capacity against nickel catalysts. In addition to this, it was reported that in terms of methane conversion and carbon capacity, once again, nickel is more active than iron on the similar support and at the similar reaction conditions.

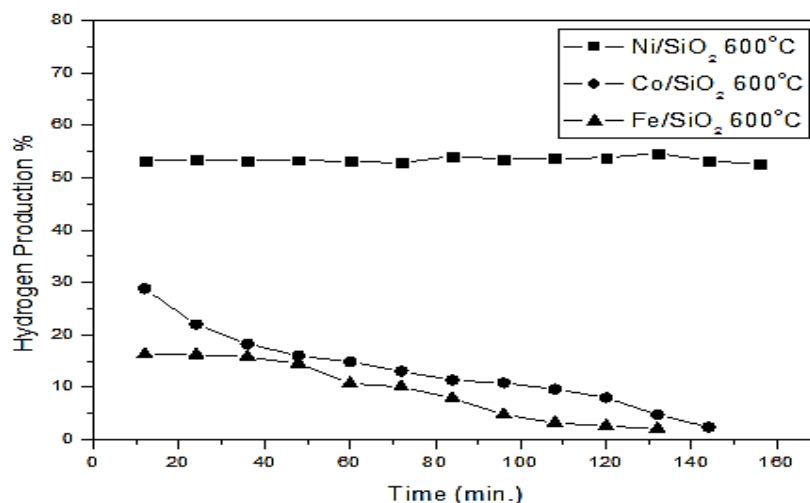


Figure 5-15: Hydrogen production efficiencies for all catalysts at 600°C

The catalysts also have different methane conversion efficiencies depending on temperature. Methane conversion efficiencies at the temperature of 550°C were given

in Figure 5.16. Cobalt catalysts had higher catalytic performance than the others. While there was no significantly difference between nickel and cobalt catalysts, iron catalysts had poorer results. The difference between cobalt and other metals could be come from its support that was described at the effect of substrate types on catalytic decomposition of methane. This finding is in agreement with Abbas's findings [80]. They recorded that the rate of methane decomposition activity by the transition metals follows the order: Co, Ru, Ni, Rh > Pt, Re, Ir > Pd, Cu, W, Fe, Mo.

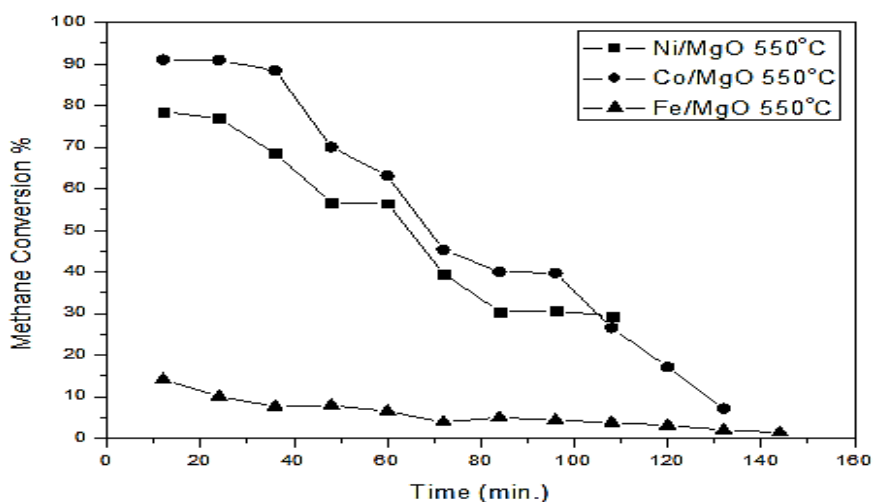


Figure 5-16: Methane conversions for all catalysts at 550°C

5.4 The Effect of Substrate Types on Catalytic Decomposition of Methane

Catalytic activity and catalyst lifetime depend strongly on the types of catalyst supports. Moreover, it is generally accepted that carbon nanotubes synthesized from catalytic decomposition process is strongly influenced by the metal-support interaction effect. Choosing the appropriate support which is complementary to the active metal is of importance in a catalyst system [66].

Among the catalyst supports, silica is the most appropriate catalyst support for the process of methane decomposition especially used with nickel. Silica supported nickel is the most active catalyst towards methane decomposition at moderate temperatures (500°C-600°C) and it has the greatest resistance towards deactivation. As shown in Figure 5.17, silica supported nickel catalyst had higher performance on hydrogen production than MgO supported nickel catalysts. Similar results existed in literature [50, 78, 81]. Takenaka et al. [50] investigated the decomposition of methane for Ni catalysts over various supports. It was concluded that SiO₂, TiO₂ and

graphite were effective supports for the catalytic decomposition of methane into hydrogen and carbon filaments. Ji et al. [81] studied the effect of nanostructured supports on catalytic methane decomposition. It was recorded that nickel was uniformly dispersed in the MgO matrix after its reduction. The highly distributed Ni could favorably stabilize high-xCH_x intermediates and therefore retard the deposition of carbon. The reason to achieve low catalytic activity using MgO support in our study could be explained by this mechanism.

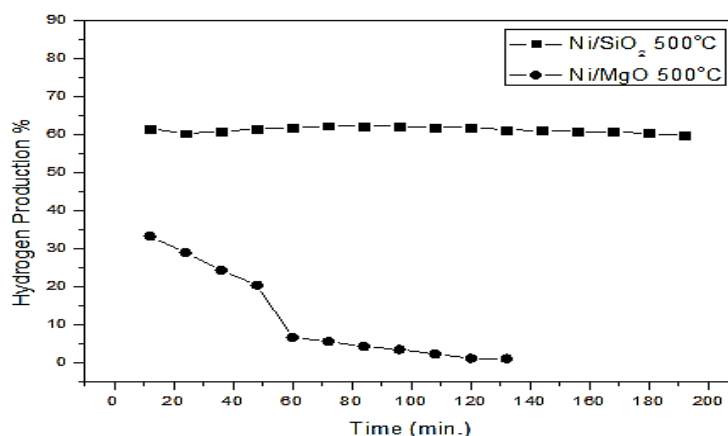


Figure 5-17: The effect of support materials on hydrogen production for Ni catalysts at 500°C

Zein et al. [78] also investigated the effect of catalyst support on the decomposition of methane to hydrogen and carbon over Cu/Ni catalysts. The results showed that the initial methane decomposition obtained within the first 5 minutes of reaction decreased in the order SiO₂ > Al₂O₃ > TiO₂ > MgO support. These data should be relatively free of deactivation effects due to blocking of active sites by the decomposition products. After 60 minutes on stream, the order of activity changed to TiO₂ > SiO₂ > MgO support. In this study, similar results were obtained from nickel catalysts data.

In contrast to Ni catalyst, the cobalt results indicated that support material of MgO gave better performance than SiO₂ (Figure 5.18). This finding is in agreement with Takenaka's [51] findings which studied the effect of supports on carbon fiber formation and hydrogen production for Co-based catalysts. The Al₂O₃ and MgO supports were found to be superior to the SiO₂ and TiO₂ supports.

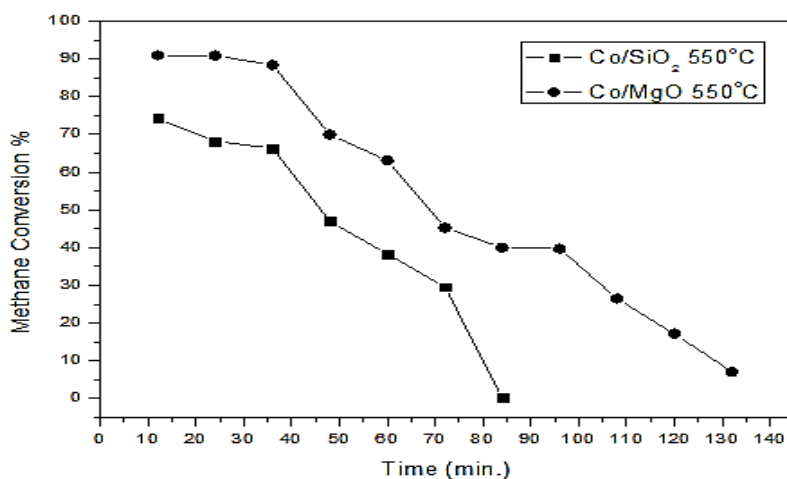


Figure 5-18: The effect of support on hydrogen production for Co catalysts at 550°C

5.5 Carbon Production Results

Carbons can be classified into different types according to their crystallinity or the degree of order, i.e., from highly ordered carbons, such as graphite and diamond, to less ordered and, finally, to disordered (amorphous and microcrystalline) carbons. It has been reported that, depending on the operating conditions of the methane catalytic decomposition process (TCD), carbon can be produced in several types: amorphous, turbostratic, and carbon fibers. Amorphous carbons are more active in methane TCD than well-ordered carbons such as graphite, diamond and carbon nanotube (CNT) because the surface concentration of high-energy sites increases with the decrease in carbon-crystallite size and conversely decreases as carbon becomes more ordered. Accordingly, the catalytic activity of carbons towards methane decomposition is in the following order: amorphous > turbostratic > graphite [80].

5.5.1 XRD results

After the thermal decomposition of methane, solid carbon was recorded by Rigaku D/Max-2200/PC diffractometer using nickel filtered Cu-K α ($\lambda=1.5418 \text{ \AA}$) radiation. The step scans by using step range as 0.02° were taken between the ranges of 2θ angles from 10° to 90° .

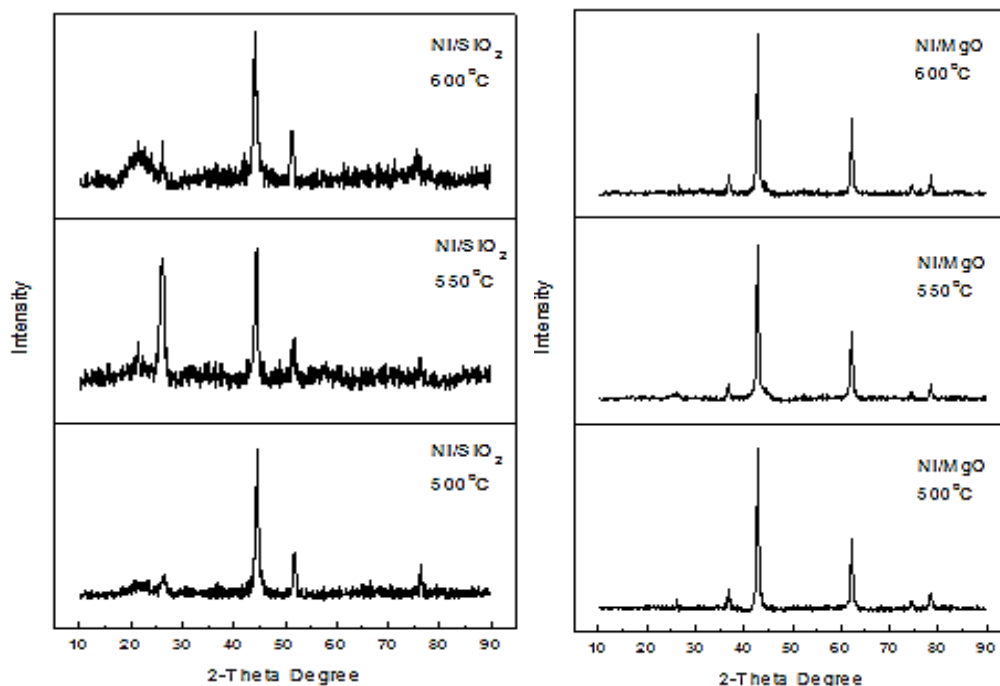


Figure 5-19: XRD patterns of deactivated nickel catalysts at various temperatures

XRD patterns of deactivated nickel catalysts were given in Figure 5.19. The irreversible carbon that was deposited on the catalyst, which was appeared in the XRD pattern of the deactivated catalysts, indicated the methane decomposition to produce hydrogen and carbon. The reflections at $2\theta = 26.40^\circ$, 26.04° and 26.06° were carbon peaks for Ni/SiO₂ at 500, 550 and 600°C respectively. It was obviously seen that nickel silica catalyst at 550°C had higher intensity for carbon peak than others.

The reflections at $2\theta = 26.06^\circ$, 26.140° and 26.68° were carbon peaks for Ni/MgO at 500, 550 and 600°C respectively. Moreover, the presence of metallic nicks in the deactivated Ni/SiO₂ catalysts reveal that the NiO phase were reduced to form metallic Ni during the pretreatment of the catalysts. The results indicated that the metallic nicks were active for the decomposition of methane. However, the reflection at $2\theta = 42.86^\circ$, 42.84° and 42.88° was related to NiO phase for Ni/MgO at 500, 550 and 600°C respectively. This might cause low carbon deposition over catalyst and it was proved with TGA and SEM data.

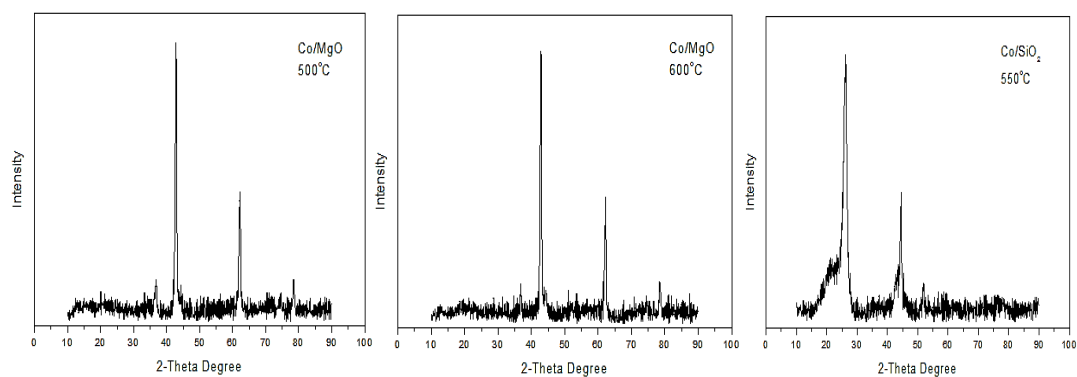


Figure 5-20: XRD patterns of deactivated cobalt catalysts at various temperatures

XRD patterns of deactivated cobalt catalysts were given in Figure 5.20. Co/SiO₂ catalysts were generally gave poor result at the temperature of 500 and 600°C for hydrogen production and solid carbon formation. However, higher methane conversion and carbon formation were observed for Co/SiO₂ catalyst at the temperature of 550°C. The reflection at $2\theta=26.12^\circ$ was carbon peak for Co/SiO₂ at 550°C. The presence of metallic cobalt in the deactivated Co/SiO₂ catalysts ($2\theta=44.52^\circ$) reveals that the CoO phase were reduced to form metallic Co during the pretreatment of the catalysts. It indicated that the metallic cobalt was active for the decomposition of methane to achieve higher methane conversions. The deposition of carbon over cobalt catalyst caused reactor clogging and deactivation. However, cobalt metal remained after decomposition reaction. It shows that methane conversion and carbon amount could be much better than these results, if the clogging was not occurred suddenly. These results were also proved by SEM and TGA data. Co/MgO catalysts gave better performance on hydrogen production than Co/SiO₂ because of the support material effect.

The reflections at $2\theta=44.40^\circ$, 74.82° and 44.04° , 74.46° were carbon peaks for Co/MgO at 500 and 600°C, respectively. The main peaks were belongs to MgO support materials as shown in Figure 5.20. Moreover, the reflections at $2\theta=36.85^\circ$ and 36.84° were cobalt oxides peaks at 500 and 600°C, respectively. This might cause low carbon deposition over catalyst and it was proved by TGA and SEM data.

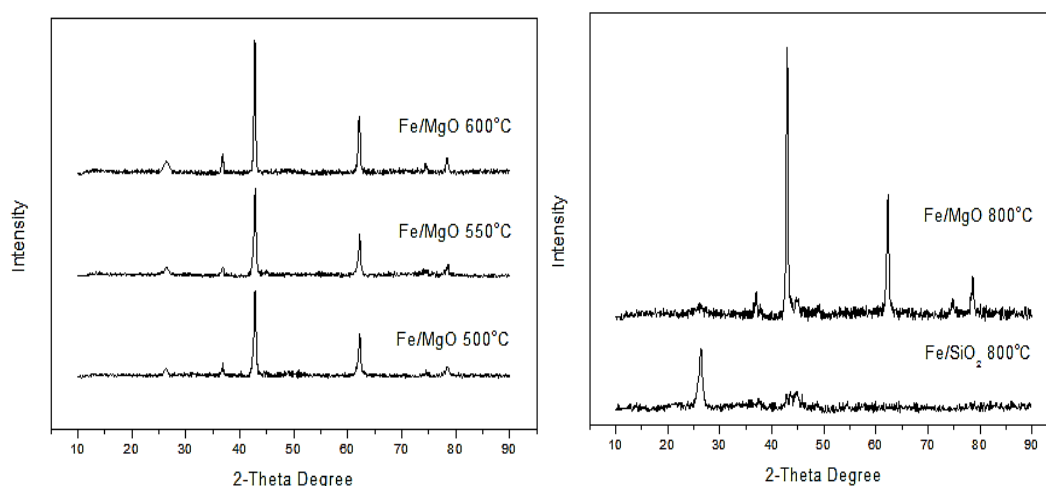


Figure 5-21: XRD patterns of deactivated iron catalysts at various temperatures

XRD patterns of deactivated iron catalysts were given in Figure 5.21. Fe/SiO₂ catalysts were generally gave poor result at the temperature of 500 to 600°C for solid carbon formations; therefore XRD analyses were not exist. However, Fe/SiO₂ catalyst at temperature of 800°C had higher methane conversion and carbon deposition as shown in Figure 5.21. The reflection at $2\theta=26.620^\circ$ was carbon peak for Fe/SiO₂ at 800°C. Carbon formation was observed at SEM and TGA analyses.

Fe/MgO catalysts had lower methane conversions than Fe/SiO₂; however, carbon depositions of Fe/MgO catalysts at the temperature of 500°C to 600°C were higher than silica supported iron catalysts that proved by SEM and TGA data. The reflections at $2\theta=26.22^\circ$, 26.30° and 26.26° were carbon peaks for Fe/MgO at 500, 550 and 600°C, respectively. The main peaks were belongs to MgO support materials as shown in Figure 5.21. In contrast to this result, Fe/MgO at the temperature of 800°C had lower carbon deposition than Fe/SiO₂ catalyst. It could be seen from XRD results that the reflection at $2\theta=26.053^\circ$ for Fe/MgO catalyst at the temperature of 800°C. Moreover, the reason of low methane conversion for Fe/MgO catalysts could be described from XRD data. The reflections $2\theta=36.90^\circ$, 36.64° , 36.78° and 37.68° were belongs to Fe₂O₃ at the temperature of 500, 550, 600 and 800 °C respectively. This indicated that the reduction was not complete properly. Therefore, catalytic activity of MgO supported iron catalysts decreased.

5.5.2 TGA results

TGA has been used to study the oxidation stability of graphite and carbon nanotubes. In order to investigate the carbon product quality, TG analyses of the deactivated catalyst samples (solid carbon and catalysts) were performed in oxygen atmosphere with a ramp of 10°C/min between 30 and 800°C. Spent catalysts were directly used for analysis without any purification process. The lines reflected the weight loss upon heating and their shape were dependent on the composition and the oxidative stability of the sample components. A final temperature of 800°C was sufficient for complete burning of the nanotubes and carbon impurities such as graphite and amorphous carbon that were completely burned at the temperatures of 520-630°C. The residual weights (%) after the heating process showed the presence of metallic impurities (Figure 5.22).

The carbon efficiency of as produced solid carbon was calculated according to TGA measurements. The dry weight percent at 200°C was selected to eliminate any losses due to existing moisture in the sample, and the final temperature is taken as 800°C to have the same temperature value for all samples. The formula of carbon efficiency is:

$$\text{Carbon efficiency(\%)} = \frac{\text{Weight \% (200°C)} - \text{Weight \% (800°C)}}{\text{Weight \% (200°C)}} \times 100 \quad (5.3)$$

In this study, TG data and carbon efficiencies were given in Figure 5.22 for nickel catalysts with different supports (SiO₂, Al₂O₃ and MgO). The weight losses step occurred for nickel silica catalysts at the temperature of 600°C due to the oxidation of carbon nanotubes. At the reaction temperature of 550°C, the weight loss was higher than other reaction temperatures and had higher carbon amount than other catalysts. This was also proved by XRD and SEM analyses. After oxidation, approximately 96, 63 and 88% of the samples were remained for Ni/SiO₂ catalyst obtained at methane decomposition temperatures of 500, 550 and 600 °C, respectively. Carbon efficiencies were calculated and Ni/SiO₂ catalyst at the temperature of 550°C had higher efficiency (36.5%). For Ni/MgO catalyst at the temperature of 550°C the carbon yield was about 14 %. Low carbon deposition could also be seen from XRD and SEM data.

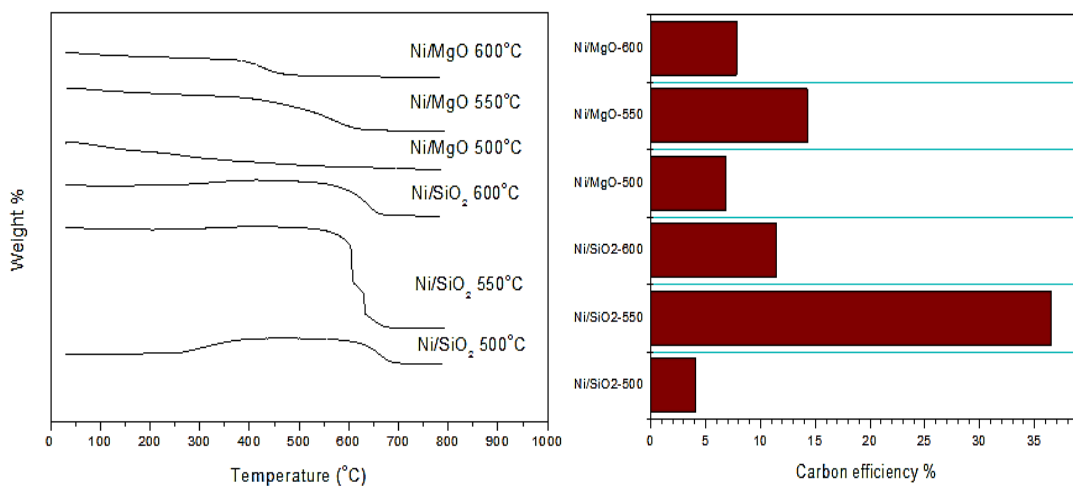


Figure 5-22: TGA of carbon materials and carbon efficiency (%) for nickel catalysts

A. Venugopal et al. [46] also investigated nickel silica catalyst over methane decomposition. It is concluded that the TG analyses of the solids under nitrogen showed several weight losses between 50 and 460°C, identified as due to water loss. The mass-loss step occurs at about 520°C accounting for the higher stability of the carbon and multi walled nature of CNTs formed. On the other hand, lower off set temperature attributed to oxidation containing amorphous carbon or CH_x species nanotubes with structural defects.

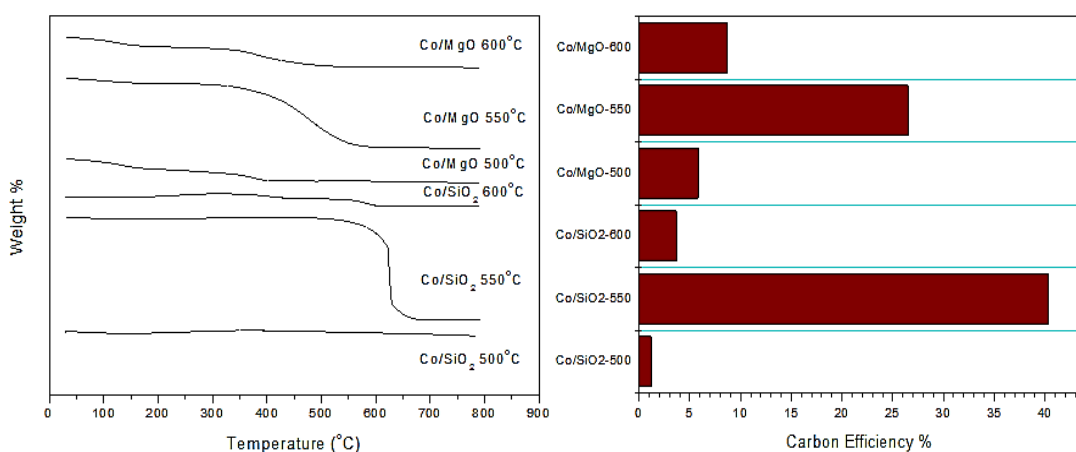


Figure 5-23: TGA of carbon materials and carbon efficiency (%) for cobalt catalysts

TG data and carbon yields for cobalt catalysts were given in Figure 5.23. Low weight losses were detected at the temperatures of 500°C and 600°C. However, the metallic impurities of deactivated catalysts at the temperature of 550°C were determined as 59 and 72 % for Co/SiO₂ and Co/MgO, respectively. Gumus et al. [75] were also studied on single-walled carbon nanotube production over different loading amounts

of Ni, Fe, and Co and Fe-Co catalysts with various substrates as SiO₂, Al₂O₃ and MgO. They found that metallic impurities of the samples were 72 and 74 % for the catalysts of Co/SiO₂, Co/MgO respectively. Avdeeva et al. [76] studied about cobalt catalysts that were tested in methane decomposition reaction at 475-600°C. It was concluded that methane conversion increased with temperature while carbon capacity and catalyst lifetime decreased. These results were also proven by carbon yields and high efficiency were observed at the temperature of 550°C. The carbon efficiencies were calculated as 40.3 and 26.5 % for Co/SiO₂ and Co/MgO respectively. In this study, the relation between methane conversion and carbon amount showed similar behavior which also proved by SEM-EDX results.

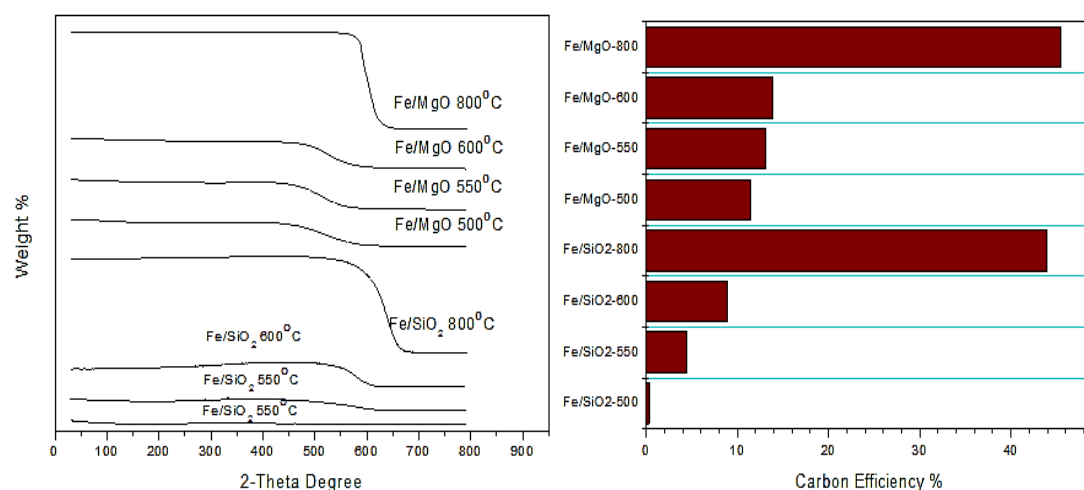


Figure 5-24: TGA of carbon materials and carbon efficiency (%) for iron catalysts

TG data and carbon yields for iron catalysts were given in Figure 5.24. It was found that metallic impurities of the samples for Fe/SiO₂ catalysts were 98, 95, 92 and 56 % at methane decomposition temperatures of 500, 550, 600 and 800°C, respectively. Moreover, for Fe/MgO, the metallic impurities of the samples were found as 87, 86, 86 and 55% at the temperatures of 500, 550, 600 and 800°C, respectively. The results of methane conversion for all catalysts were proved by TG analyses and carbon efficiencies (%). For iron catalysts at methane decomposition temperature of 800°C, the carbon efficiencies were calculated as 43 and 45 % for Fe/SiO₂ and Fe/MgO, respectively. The deactivated catalyst samples demonstrated high residual weight belonging to catalyst particles. Similar results were obtained in literature studies [67, 75]. Gumus et al. [75] were found that metallic impurities of the samples were 69 and 80 % for the catalysts of Fe/SiO₂ and Fe/MgO, respectively. Moreover, Pinilla

et. al [67] investigated Ni and Fe based catalysts for hydrogen and carbon nano filament production by catalytic decomposition of methane in a rotary bed reactor. They were achieved 70% weight loss by using Mo doped Fe/MgO catalyst. It was concluded that the residual weight (due to the amount of metal catalyst present) was higher than Fe-based catalysts. A possible explanation concerning the better behavior of the Fe.Mo/MgO catalysts in terms of both hydrogen production and quality of the carbonaceous product could be the interaction of iron particles with Mo which prevents iron particles from agglomerating at reduction and reaction conditions.

5.5.3 SEM results

Solid carbon samples were examined by SEM (Philips XL30 SFEG) at an accelerating voltage of 15 kV. Elemental compositions of the catalysts were determined by energy-dispersive X-ray spectroscopy (EDX).

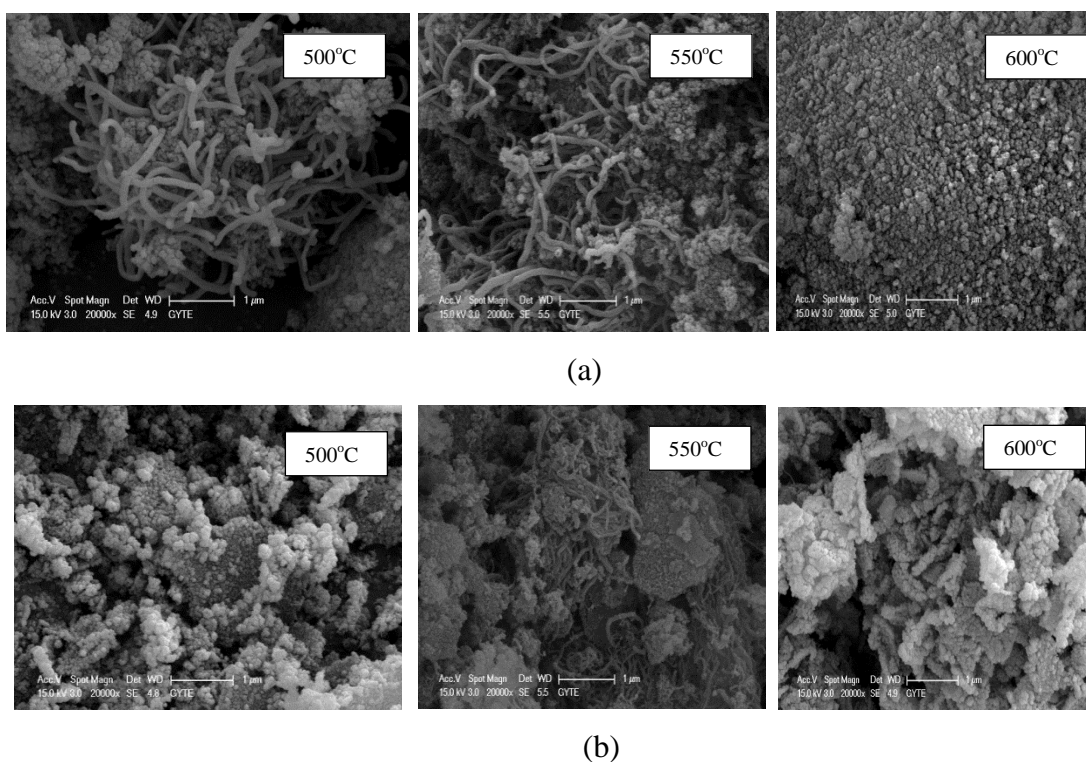


Figure 5-25: SEM images of CNTs produced using (a) Ni/SiO₂ and (b) Ni/MgO catalysts

Micrographs of the carbon samples produced using the catalysts of Ni/SiO₂ and Ni/MgO at the temperatures of 500 and 550°C were given in Figure 5.25. It is seen from this figure that the surface is partially covered with filamentous carbon, in

contrast to the clean surface seen in the fresh catalysts during decomposition of methane. As illustrated by the micrographs, most of this carbon is in the form of potentially valuable carbon filaments. For other catalysts, filamentous carbon was not seen on catalysts surfaces as shown in Figure 5.25. However, the weight percentages of carbon samples were analyzed as 27, 30 and 22 % for Ni/SiO₂ at the temperatures of 500, 550 and 600°C by using EDX analyses respectively. Moreover, the carbon weights of Ni/MgO catalysts at the temperatures of 500, 550 and 600°C were found as 28, 14 and 22 %, respectively. The result of low carbon deposition on Ni/MgO catalysts was that the nickel oxide could not be converted to nickel metals due to low reduction temperature. SEM results are in agreement with XRD and TG results. Another differential feature from SEM micrographs is that the abundance of bright areas, which are due to the bare Ni surfaces. As shown in Figure 5.25, after the reaction time of 3h, there were also bright areas over deactivated catalysts that showed active Ni metals to produce hydrogen.

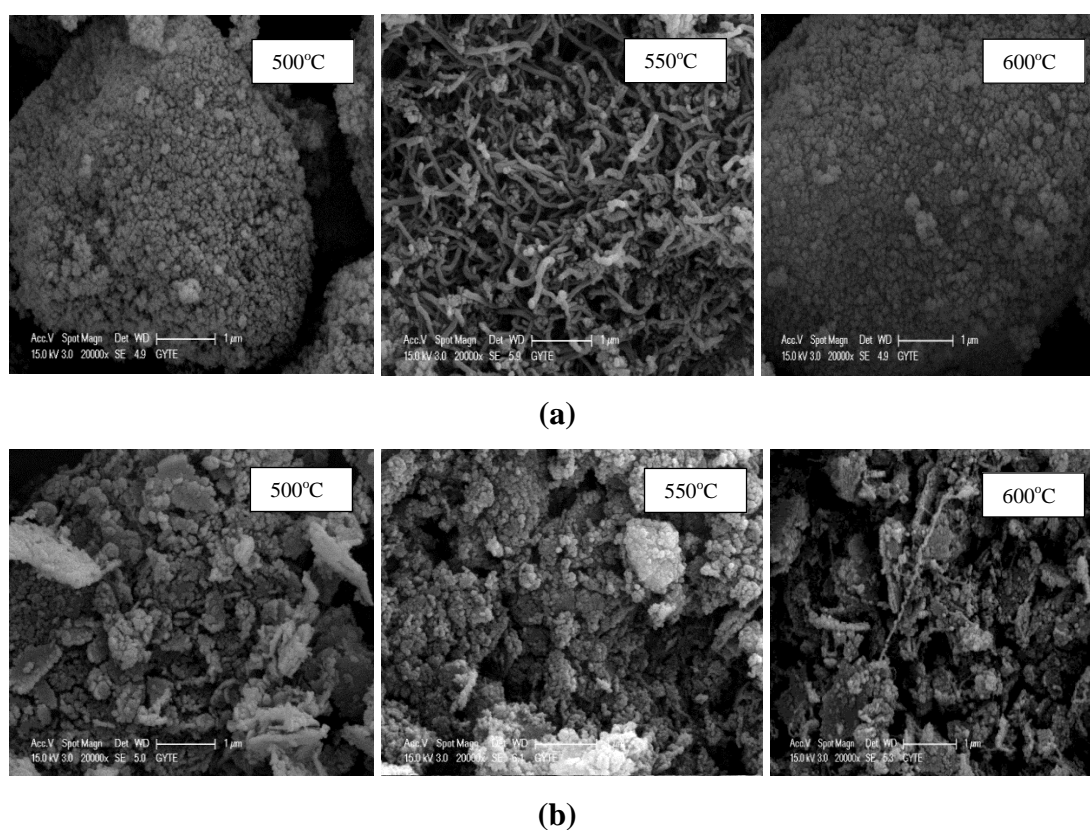
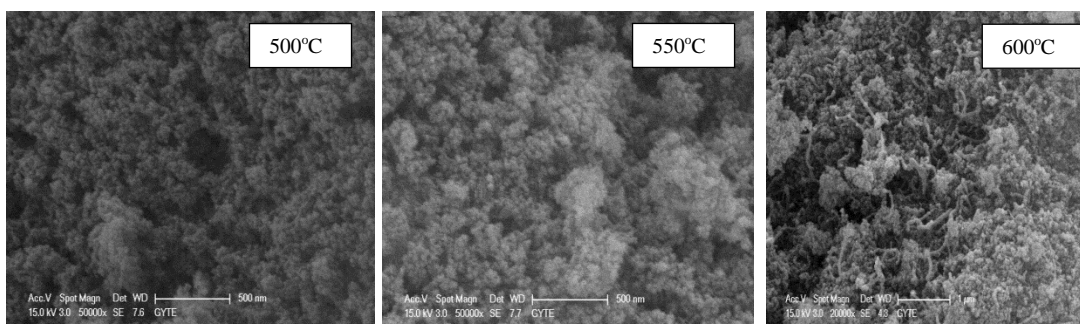
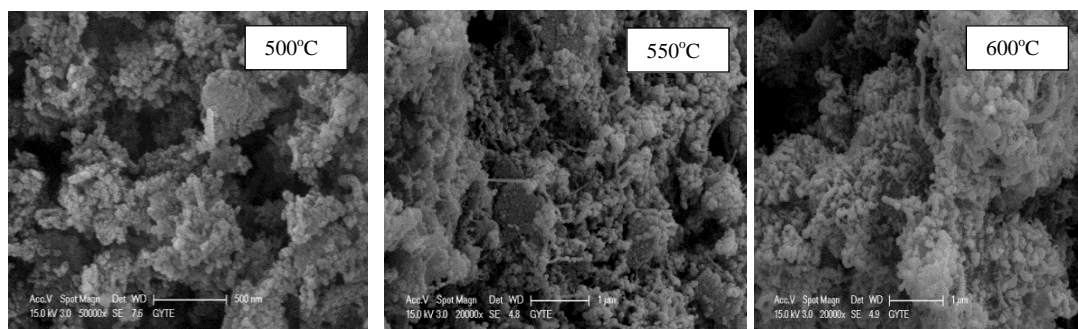


Figure 5-26: SEM images of CNTs produced using (a) Co/SiO₂ and (b) Co/MgO catalysts

The SEM images of carbon nanotubes produced by cobalt catalysts are shown in Figure 5.26. As illustrated by the figure, most of this carbon is in the form of valuable carbon filaments. The weight percentages of carbon samples for Co/SiO₂ catalyst were analyzed by using EDX analyses and found as 24, 79 and 31 % at methane decomposition temperatures of 500, 550 and 600 °C respectively. Moreover, for Co/MgO catalysts, the weight percentages were determined as 14, 39 and 22 % at the temperatures of 500, 550 and 600 °C, respectively. As shown in Figure 5.26, the surfaces of cobalt catalysts were covered by filamentous carbon at 550 °C which proved with TG analyses. Co/MgO catalyst showed better performance on methane decomposition and carbon production than Co/SiO₂ catalysts. This difference could be explained by support material effect. Similar results were obtained in Chai et al.'s study [66]. They stated that MgO as a catalytic support has widely been studied due to the advantages over Al₂O₃ and SiO₂: MgO can be easily dissolved in acid and that simplifies the carbon nanotubes purification steps. Besides that, MgO supported Co is capable in producing SWNTs. Nevertheless, metals supported on MgO showing low catalytic activity (except cobalt metal) towards decomposition of methane and this reason impels the researches to search the suitable transition metals supported on MgO for effective SWNTs production. Furthermore, temperature changes affect the type of carbon deposition. At constant reaction temperature of 1000 °C SWNTs can be produced in abundance over Co/MgO, and reaction temperature over or below 1000 °C would lead to the formation of other materials such as MWNTs and amorphous carbon.



(a)



(b)

Figure 5-27: SEM images of CNTs produced using (a) Fe/SiO₂ and (b) Fe/MgO catalysts

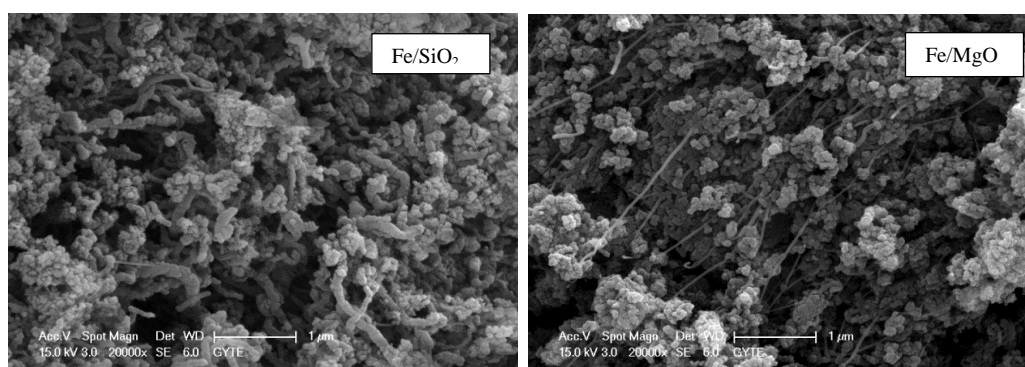


Figure 5-28: SEM images of CNTs synthesized using iron catalysts at the temperature of 800 °C

The SEM images of carbon nanotubes synthesized by iron catalysts are shown in Figure 5.27 and Figure 5.28. Fe/SiO₂ catalysts at methane decomposition temperatures of 500, 550 and 600°C gave poor result on carbon nanotube formations that was also proved by TG data. Ermakova et al. [52] stated that silicate can either inhibit or promote formation of carbon depending on their amount comprised in Fe/SiO₂ catalysts. In spite of that Fe/MgO catalysts showed high performance on carbon deposition although having low methane conversions. Moreover, the material obtained from methane decomposition using Fe/MgO consisted of more homogeneous nano-filaments. The surface of Fe/SiO₂ catalyst at the temperature of 800°C was covered with carbon nanotubes shown in Figure 5.28. It is seen from the figure that most of this carbon is in the form of potentially valuable carbon filaments. EDX analyses were also performed for each catalyst. The results indicated that carbon contents as weight percentage were 23 % for Fe/MgO and 55 % for Fe/SiO₂. These results were supported by TG and SEM data.

6. OVERALL RESULTS AND RECOMMENDATIONS

In this study, the catalytic decomposition of methane was investigated through a fixed-bed vertical stainless steel reactor using different catalyst (Fe, Ni and Co), support materials (MgO and SiO₂) under different temperatures (500-600°C). Furthermore, the production of an available solid form of by-product carbon via catalytic decomposition of methane was examined. The catalysts and by-product carbon materials were characterized by XRD, TEM and SEM techniques.

6.1 Concluding Remarks

1. It was observed that with the change of the particle size in catalyst, the methane conversion and carbon deposition efficiencies were changed. While nickel particle size over silica support was in the range that given from literature to obtain high efficiency, nickel particle size over MgO support was not in the range; as a result of this, it gave poor results on methane conversion and carbon deposition.
2. The reaction temperature is one of the most important parameters influencing the catalyst activity, catalyst lifetime. While the methane conversion is increased, the catalyst lifetime is decreased.
3. Ni/SiO₂ catalyst at the temperature of 500°C gave better performance on methane conversion than the other temperatures. It was stabilized during the reaction time of 3h. However, at the temperature of 550°C, catalyst had higher carbon deposition potential.
4. Ni/MgO catalyst at the temperature of 500 and 600°C gave lower performance on methane conversion than the reaction temperature of 550°C during the reaction time of 3h. Ni/MgO catalyst also had lower carbon deposition than Ni/SiO₂ catalyst.
5. Co/SiO₂ catalyst at the temperature of 550°C had higher methane conversion and carbon deposition efficiency than other temperatures.

6. Co/MgO catalyst gave better performance on hydrogen production efficiencies than Co/SiO₂ for all temperatures. The best result of Co/MgO catalyst was obtained at the temperature of 600°C.
7. As the temperature was increased, methane conversion and carbon deposition were increased for Fe/SiO₂ and Fe/MgO. There was no significantly difference on hydrogen production efficiencies at lower temperatures (500-600°C). However, the temperature was increased to 800°C; Fe/SiO₂ catalyst was superior to Fe/MgO catalysts on methane conversion efficiency.
8. The reduction temperature effect was also studied for iron catalysts. It was concluded that as the reduction temperature was increased, the methane conversion and carbon deposition was increased. The suitable reduction temperature should be chosen to obtain high yield hydrogen and solid carbon.
9. The catalytic activity of silica supported catalysts was ordered as; Ni>Co>Fe at all temperatures. However, the catalytic activity of MgO supported catalyst were ordered as Co>Ni>Fe.
10. The effect of support materials were investigated in this study. The order of methane conversion efficiencies was SiO₂>MgO.
11. The surface of Ni/SiO₂ catalyst was partially covered with filamentous carbon, in contrast to the clean surface seen in the fresh catalysts during decomposition of methane. For Ni/MgO catalysts, filamentous carbon was not seen on catalysts surfaces at the temperature of 550°C.
12. Co/SiO₂ catalyst at the temperature of 550°C gave better performance than Co/MgO. The filamentous carbon was covered to catalyst surface. However, other temperatures for Co/SiO₂ had poorer results on carbon deposition. Moreover, it was concluded that temperature changes affect the type of carbon deposition.
13. Fe/SiO₂ catalysts at the temperature of 500, 550 and 600°C gave poor results on carbon nanotube formations. Fe/MgO catalysts showed high performance on carbon deposition although having low methane conversions. It was concluded that silicate could inhibit or promote formation of carbon depending on their amount comprised in Fe/SiO₂ catalysts.

14. The carbon efficiencies were calculated as 43 and 45 % at methane decomposition temperature of 800°C for Fe/SiO₂ and Fe/MgO, respectively.

15. Carbon efficiencies for Ni/SiO₂ catalyst at methane decomposition temperature of 550°C had higher efficiency (36.5%). For Ni/MgO catalyst at the temperature of 550°C the carbon yield was about 14 %.

16. The carbon efficiencies were also calculated as 40.3 and 26.5 % at methane decomposition temperature of 550°C for Co/SiO₂ and Co/MgO, respectively.

6.2 Recommendations

The methane conversion and carbon efficiencies of the various metal catalysts used in this study shows differences from the previously conducted researches in the literature. These differences are mainly due to reaction temperatures and preparation of catalyst. In the further studies:

- The different catalyst preparation methods (wetness impregnation, precipitation, sol-gel technique) except the method applied in this thesis can be conducted.
- The different substrate materials (alumina, titanium dioxide, etc.) other than SiO₂ and MgO can be examined.
- Binary catalyst or different monometallic catalysts can be used in the catalytic decomposition of methane.
- The different hydrocarbon source (ethylene, propane etc.) can be used in the catalytic decomposition of methane.
- The fluidized bed reactor can be used for decomposition of methane to increase efficiency of hydrogen and also carbon formation.
- The other reaction conditions (reduction temperature, reaction temperature, gas velocity, etc.) can be changed to observe the effects of these parameters on hydrogen and solid carbon production.

REFERENCES

- [1] **College of Desert** (2001). *Hydrogen Fuel Cell Engines and Related Technologies: Module 1 Hydrogen Properties*.
- [2] **Gupta, R.B.** (2008). *Hydrogen Fuel Production, Transport and Storage*, CRC Press.
- [3] **Royal Belgian Academy Council of Applied Science** (2006). *Hydrogen as an energy carrier*.
- [4] **Muradov, N., Smith, F. and Raissi, A.** (n.d.). *Dissociation of Hydrocarbons: a Route to CO-free Hydrogen*, Florida Solar Energy Center, University of Central Florida, U.S.A.
- [5] **Yürüm, Y.** (n.d.). *Hydrogen Energy System Production and Utilization of Hydrogen and Future Aspects*, Department of Chemistry, Hacettepe University, Ankara, Turkey.
- [6] **Shah, N., Ma, S., Wang, Y., Gerald, P.** (2007). Semi-continuous hydrogen production from catalytic methane decomposition using a fluidized-bed reactor, *International Journal of Hydrogen Energy*, Volume 32, Issue 15, Pages 3315–3319.
- [7] **Muradov, N., Smith, F., and Raissi, A.** (2005). Catalytic activity of carbons for methane decomposition reaction, *Catalysis Today*, volumes 102–103, Pages 225–233.

- [8] **HF, A., Wmaw, D.** (2009). Deactivation of palm shell-based activated carbon catalyst used for hydrogen production by thermo-catalytic decomposition of methane, *International J. Hydrogen Energy*, 34(15):6231–41.
- [9] **Palmer, D.** (2008). Hydrogen in the Universe. NASA. Retrieved from http://imagine.gsfc.nasa.gov/docs/ask_astro/answers/971113i.html.
- [10] **Othmer, K.** (1992). *Encyclopedia of Chemical Technology*, 3rd ed., Vol. 4, Wiley, New York, 631p.
- [11] **Gurov, Y.B., Aleshkin, D.V., Behr, M.N., Lapushkin, S.V., Morokhov, P.V., Pechkurov, V.A., Poroshin, N.O., Sandukovsky, V.G., Tel'kushev, M.V., Chernyshev, B.A., Tschurenkova, T.D.** (2004). Spectroscopy of super heavy hydrogen isotopes in stopped pion absorption by nuclei. *Physics of Atomic Nuclei*, 68 (3): 491–97.
- [12] **Hydrogen plant Design, Properties and Uses of Hydrogen**, Url <http://www.sbioinformatics.com/design_thesis/Hydrogen/Hydrogen_Properties&uses..pdf> ,
- [13] **Brinner, A. and Philipps F.** (n.d.). *Hydrogen as the fuel of the future-production; purification; storage*. Institute for technical thermodynamics German aerospace center, Stuttgart
- [14] **Momirlan, M. and Veziroglu. T.N.** (2005). The properties of hydrogen as fuel tomorrowin sustainable energy system for a cleaner planet, *International Journal of Hydrogen Energy*, 795 – 802.
- [15] **White, C.M., Steeper R.R. and Lutz, A.E.** (2006). “The hydrogen fueled internal combustion engine:A technical review.” *Int. J. Hydrogen Energy*, 31, 1292–1305.

- [16] **Riis, T., Hagen, E.F., Vie, P.J.S. and Ulleberg, O.** (n.d.). “Hydrogen Production R&D: Priorities And Gaps”, *International Energy Agency*, Hydrogen Implementing Agreement
- [17] **Evenson, W.E.** (n.d.). *R &D of Energy Technologies*, Annex A Iv Hydrogen Energy, retrieved from <http://www.iupap.org/wg/energy/annex-1d.pdf>.
- [18] **Dinçer, İ.** (2012). Green methods for hydrogen production, Faculty of Engineering and Applied Science, University of Ontario Institute of Technology, 2000 Simcoe Street North, Oshawa, ON L1H 7K4, Canada. *International journal of hydrogen energy*, 37:1954-1971
- [19] **Muradov, N., Smith, F., Huang, C. and T-Raissi A.** (2006). Autothermal catalytic pyrolysis of methane as a new route to hydrogen production with reduced CO₂ emissions, *Catalysis Today*, 116:281–288.
- [20] **National Research Council.** (2004). *The hydrogen economy: opportunities, costs, barriers and R&D Needs*, National Academies Press, Washington.
- [21] **The National Hydrogen Energy Roadmap .** (2002), *National Hydrogen Energy Roadmap Production, Delivery, Storage, Conversion, Applications, Public Education And Outreach*, Washington, DC.
- [22] **European Commision.** (2003), *Hydrogen Energy and Fuel Cells: A vision of our future*, Directorate-General for Research, Directorate-General for Energy and Transport EUR 20719.
- [23] **Url** <<http://psipunk.com/future-cars-the-hydrogen-cars-technology/>>, date retrieved 18.11.2013.
- [24] **Url** <<http://auto.howstuffworks.com/fuel-efficiency/hybridtechnology/hydrogen-cars1.htm>>, data retrieved 19.11.2013.

- [25] **Yazici, M.S.** (2012), World Hydrogen Energy Conference 2012 Hydrogen and fuel cell educational activities in Turkey, *Energy Procedia*, 29:690 – 694.
- [26] **Rand, D.A.J.** (n.d.), *Hydrogen Energy Challenges and Prospects*, CSIRO Energy Technology, Victoria, Australia R.M. Dell Formerly Head of Applied Electrochemistry, Atomic Energy Research Establishment, Harwell, UK
- [27] **Molburg, J.C. and Richard, D.** (2003), *Hydrogen from Steam-Methane Reforming with CO₂ Capture*, 20th Annual International Pittsburgh Coal Conference, September 15-19, Pittsburgh, PA
- [28] **Beurden, P.V.** (2004). *On the Catalytic Aspects of Steam-Methane Reforming; A Literature Survey*. Retrieved from <http://www.ecn.nl>, ECN Report ECN-I-04-003.
- [29] **Rostrup, J. and Hansen, J.B.** (1993), CO₂-reforming of methane over transition metals, *Journal. Catalysis*, pg.144.
- [30] **Bej, B., Pradhan, N.C. and Neogi, S.** (2012), Production of hydrogen by steam reforming of methane over alumina supported nano-NiO/SiO₂ catalyst, *Catalysis Today*, 207: 28– 35.
- [31] **Wang, H.Y. and Ruckenstein, E.** (2001), Partial oxidation of methane to synthesis gas over alkaline earth metal oxide supported cobalt catalysts, *Journal Catalysis*, 199:309–17.
- [32] **Zeman, H., Url, M. and Hofbauer, H.** (n.d.), *Autothermal Reforming of Hydrocarbon Fuels*, Institute of Chemical Engineering, Vienna University of Technology.

- [33] **Zhang, M., Cheng, D. and Zhang, Y.** (n.d.). *Carbon Dioxide Reforming of Methane over a Novel Ni/Al₂O₃ Catalysts*, Key Laboratory of Green Chemical Technology of Ministry of Education, School of Chemical Engineering, Tianjin University.
- [34] **Pena, J.A., Lorente, E. and Herguido, J.** (n.d.). *Steam-Iron Process for Hydrogen Production: Recent Advances Catalysis*, Molecular Separations and Reactor Engineering Group (CREG), Aragón Institute of Engineering Research, Universidad de Zaragoza, Spain
- [35] **Labrecque, R. and Lafl, A.** (2002). *Electricity-assisted syngas generation, Report*, Hydro Quebec Institut de Recherche.
- [36] **Okabe, H.** (1978). *Photochemistry of Small Molecules*, Chap. 7, Wiley, New York.
- [37] **Muradov, N.** (2002). *Thermo-catalytic CO₂-Free Production of Hydrogen from Hydrocarbon Fuels*, Proceedings of the U.S. DOE Hydrogen Program Review NREL/CP-610-32405.
- [38] **Muradov, N. and Veziroglu, T.** (2005). From hydrocarbon to hydrogen–carbon to hydrogen economy, *Intl. J. Hydrogen Energy*, 30:225–237.
- [39] **Choudhary, T.V. and Goodman, D.W.** (2006). Methane Decomposition: Production of Hydrogen and Carbon Filaments, *Catalysis RSC*, 19, 164–183.
- [40] **Ahmeda, S., Aitani, A., Rahman, F., Al-Dawood, A. and Al-Muhaish, F.** (2009). Review, Decomposition of hydrocarbons to hydrogen and carbon, *Applied Catalysis A: General*, 359:1–24
- [41] **Snoeck, J., Froment, G., and Fowles, M.** (1997), Kinetic study of the carbon filament formation by methane cracking on a nickel catalyst, *J. Catalysis.*, 169; 250.

- [42] **Koerts, T., Deelen, M., and van Santen, R.** (1992), Hydrocarbon formation from methane by a low temperature two-step reaction sequence, *J. Catalysis*, 138;101.
- [43] **Avdeeva, L.B., Reshetenko, T.V., Ismagilov, Z.R. and Likholobov, V.A.** (2002), Iron-containing catalysts of methane decomposition: accumulation of filamentous carbon, *Applied Catalysis A*; 228:53-63.
- [44] **Ermakova, M.A., Ermakov, D.Y. and Kuvshinov, G.G.** (2000), Effective catalysts for direct cracking of methane to produce hydrogen and filamentous carbon: Part I. Nickel catalysts, *Applied Catalysis A*; 201:61-70.
- [45] **Parmon, V.** (2005), Hydrogen Production and Fuel Cells, *Presented at the ICS Meeting*, Trieste, Italy.
- [46] **Venugopal, A., Kumar, S.N., Ashok, J., Prasad, D.H., Kumari, V.D., Prasad, K.B.S, Subrahmanyam, M.** (2007), Hydrogen production by catalytic decomposition of methane over Ni/SiO₂, *International Journal of Hydrogen Energy*, 32 1782 – 1788.
- [47] **Chesnokov, V.V. and Chichkan A.S.** (2009), Production of hydrogen by methane catalytic decomposition over Ni-Cu-Fe/Al₂O₃ catalyst, *Int J Hydrogen Energy*, 34:2979-2985.
- [48] **Shah, N., Panjala, D. and Huffman, G.P.** (2001), Hydrogen production by catalytic decomposition of methane, *Energy and Fuels*, 15;1528-1534.
- [49] **Pinilla, J.L., Utrilla, R., Karn, R.K., Suelves, I., Lazaro, M.J., Moliner, R., Garcı, A.B. and Rouzaud. J.N.** (2011), High temperature iron-based catalysts for hydrogen and nanostructured carbon production by methane decomposition, *International journal of hydrogen energy*, 36;7832-7843.

- [50] **Takenaka, S., Ogihara, H., Yamanaka, I. and Otsuka, K.** (2001). Decomposition of methane over supported-Ni catalysts: effects of the supports on the catalytic lifetime, *Applied Catalysis A: General*, 217;101–110.
- [51] **Takenaka, S., Ishida, M., Serizawa, M., Tanabe, E. and Otsuka, K.** (2004). Formation of carbon nanofibers and carbon nanotubes through methane decomposition over supported cobalt catalysts, *J. Phys. Chem. B*, 108;11464–11472.
- [52] **Ermakova, M.A. and Ermakov, D.Yu.** (2002), Ni/SiO₂ and Fe/SiO₂ catalysts for production of hydrogen and filamentous carbon via methane decomposition, *Catalysis Today*, 77;225–235.
- [53] **Zhang T., Amiridis M.D.** (1998), Hydrogen production via the direct cracking of methane over silica-supported nickel catalysts, *Applied Catalysis A*; 167:161-172.
- [54] **Mezaliraa, D.Z., Probst, D.L., Pronierb, S., Batonneaub, Y. and Batiot-Dupeyrat, C.** (2011), Decomposition of ethanol over Ni/Al₂O₃ catalysts to produce hydrogen and carbon nanostructured materials” *Journal of Molecular Catalysis A: Chemical*, 340;15–23.
- [55] **M. Amiridis, C. Bernales.** (1999), WO Patent 99/43609.
- [56] **Aiello, R., Fiscus, J., Loye, H. and Amiridis, M.** (2000), Hydrogen production via the direct cracking of methane over Ni/SiO₂: Catalyst deactivation and regeneration, *Applied Catalysis. A: Gen.*, 192;227–234.
- [57] **Chin, S., Chin, Y. and Amiridis, M.** (2006), Hydrogen production via the catalytic cracking of ethane over Ni/SiO₂ catalysts, *Applied Catalysis. A: General*, 300;8–13.

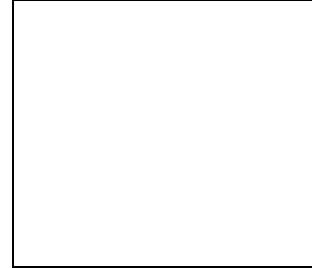
- [58] **Ammendola, P., Chirone, R., Ruoppolo, G. and Russo, G.** (2007), Regeneration of deactivated catalysts for TCD process by carbon oxidation in fluidized bed reactors, *Third European Combustion Meeting ECM*.
- [59] **Steinfeld, A., Kirillov, V., Kuvshinov, G., Mogilnykh, Y., Reller, A.** (1997), Production of filamentous carbon and hydrogen by solar thermal catalytic cracking of methane, *Chemical Engineering Science*, 52(20):3599–603.
- [60] **Muradova, N., Smitha, F., Bockermana, G. and Scammon, K.** (2009), Thermocatalytic decomposition of natural gas over plasma-generated carbon aerosols for sustainable production of hydrogen and carbon, *Applied Catalysis A: General*, 365:292–300.
- [61] **Aiello, R., Fiscus, J.E., Loye, H.Z. and Amiridis, M.D.** (2000), Hydrogen production via the direct cracking of methane over Ni/SiO₂: catalyst deactivation and regeneration, *Applied Catalysis A*, 192(2):227–34.
- [62] **Amin, A.M., Croiset, E., Malaibari, Z. and Epling, W.** (2012), Hydrogen production by methane cracking using Ni-supported catalysts in a fluidized bed, *International journal of hydrogen energy*, 37:10690-10701.
- [63] **Echegoyen, Y., Suelves, I., Lazaro M.J., Moliner, R. and Palacios, J.M.** (2007), Hydrogen production by thermo-catalytic decomposition of methane over Ni.Al and Ni.Cu.Al catalysts: effect of calcination temperature, *J Power Sources*, 169:150-157
- [64] **Baker, R.T.K.** (1989), Catalytic growth of carbon filaments, *Carbon*, 27: 315–323.

- [65] **Cassel, A.M., Raymake, A., Kong, J. and Dai, H.** (1999), Large scale CVD synthesis of single-walled carbon nanotubes, *J Phys Chem B*, 103:6484–6492.
- [66] **Chai, S.P., Zein, S.H.S. and Mohamed, A.R.** (n.d.). A Review on Carbon Nanotubes Production via Catalytic Methane Decomposition, 1st National Postgraduate Colloquium School of Chemical Engineering, USM.
- [67] **Pinilla, J.L., Utrilla, R., Lazaro, M.J., Moliner, R., Suelves L. and Garcia, A.B.** (2011), Ni- and Fe-based catalysts for hydrogen and carbon nanofilament production by catalytic decomposition of methane in a rotary bed reactor, *Fuel Processing Technology*, 92;1480–1488.
- [68] **Deminsky, M., Jivotov, V., Potapkin, B. and Rusanov, V.** (2002), Plasma-assisted production of hydrogen from hydrocarbons, *Pure Appl. Chem.*, Vol. 74, No. 3, pp. 413–418.
- [69] **Paulmier, T. and Fulcheri, L.** (2005), Use of non-thermal plasma for hydrocarbon reforming, *Chemical Engineering Journal*, 106;59–71
- [70] **Graff, M.D. and McHenry, M.E.** (2007), *Structure of Materials, An introduction of crystallography, diffraction and symmetry*, Cambridge University Press, UK.
- [71] **Ahmed, S., Aitani, A., Rahman, F., Al-Dawood, A., Al-Muhaish, F.** (2009), Decomposition of hydrocarbons to hydrogen and carbon: Review, *Applied Catalysis A: General*, 359;1–24
- [72] **Tapia-Parada, K., Valverde-Aguilar, G., Mantilla, A., Valenzuela, M.A. and Hernandez, E.** (2013), Synthesis and characterization of Ni/Ce–SiO₂ and Co/Ce–TiO₂ catalysts for methane decomposition, *Fuel*, Volume 110, Pages 70–75.

- [73] **Saraswat, S.K. and Pant, K.K.** (2013), Synthesis of hydrogen and carbon nanotubes over copper promoted Ni/SiO₂ catalyst by thermo-catalytic decomposition of methane, *Journal of Natural Gas Science and Engineering*, 13; 52-59.
- [74] **Li N., Wang X., Derrouiche S., Haller G.L., and Pfefferle L.D.** (2010), Role of Surface Cobalt Silicate in Single-Walled Carbon Nanotube Synthesis from Silica-Supported Cobalt Catalysts, *ACS Nano*, 4(3):1759-67.
- [75] **Gumus F.** (2013), Carbon nanotube synthesis with different support materials and catalysts, ITU Master Thesis.
- [76] **Avdeeva, L.B., Kochubey, D.I. and Shaikhutdinov, S.K.** (1999), Cobalt catalysts of methane decomposition: accumulation of the filamentous carbon, *Applied Catalysis A: General*, Volume 177, Issue 1, Pages 43–51.
- [77] **Wojciech, G., Andrzej D., Tadeusz B., Leszek K.** (2009), Methane decomposition over Ni–MgO–Al₂O₃ catalysts, *Applied Catalysis A: General*, 357: 236–243
- [78] **Zein S.H.S. and Mohamed, A.R.** (2004), The effect of catalyst support on the decomposition of methane to hydrogen and carbon, *HUM Engineering Journal*, Vol. 5, No. 1.
- [79] **Prabhas, J., Victor, A., Juan, M.C., Serrano, D.P.** (2010), Cobalt based catalysts prepared by Pechini method for CO₂-free hydrogen production by methane decomposition, *International Journal of Hydrogen Energy*, 35: 10285-10294.
- [80] **Abbas, H.F., Daud, W.M.A.W.** (2009), Deactivation of palm shell-based activated carbon catalyst used for hydrogen production by thermocatalytic decomposition of methane, *International Journal Hydrogen Energy*, 34(15):6231–41.

- [81] **Ji L., Tang, S., Chen, P., Zeng, H.C., Lin, J. and Tan, K.L.** (2000), Effect of nano structured supports on catalytic methane decomposition, *Pure Applied Chemistry*, Vol. 72, Nos. 1–2, pp. 327–331.

CURRICULUM VITAE



Name Surname: Cansu Deniz

Place and Date of Birth: Istanbul, 02.01.1988

Address: Göztepe/İstanbul

E-Mail: cansudenizz@yahoo.com

B.Sc.: Marmara University, Environmental Engineering and Mechanical Engineering

Professional Experience and Rewards:

Yalova University, Energy System Engineering, Research Assistant

Marmara University, Environmental Engineering, 2nd rank

List of Publications:

Deniz C., Karatepe N., “Hydrogen Production via Catalytic Decomposition of Methane: Review”, Geographical and Geocological Research of Ukraine and Adjacent Territories, 2-7 Nisan 2013, Simferopol, Ukraine

Deniz C., KARATEPE N., “Hydrogen and carbon nanotube production via catalytic decomposition of methane”, SPIE Optics & Photonics, 25-29 Ağustos 2013, San Diego, USA.

PRESENTATIONS ON THE THESIS

Deniz C., KARATEPE N., “Hydrogen and carbon nanotube production via catalytic decomposition of methane”, SPIE Optics & Photonics, 25-29 Ağustos 2013, San Diego, USA.

